BIOMEDICAL ENGINEERING MSc PROGRAM
UNIVERSITY OF CRETE
TECHNICAL UNIVERSITY OF CRETE
FOUNDATION FOR RESEARCH AND TECHNOLOGY-HELLAS

University of Crete

School of Medicine

"Biomedical Engineering"

M.Sc. Thesis

PML-mediated Glioblastoma Growth Dynamics: Insights from Spheroid-Based Studies and Brain Tissue Slice Implantation

Makrygiannaki Eirini

Supervisor: **Sakkalis Vangelis**, Research Director, FORTH-ICS

Heraklion,2024

στους γονείς μου

CONTENTS

1. ABSTRACT

Glioblastoma (GBM) is the most malignant brain cancer among adults, according to the World Health Organization (WHO). It is characterized by excessive proliferation and infiltration, along with extensive inter- and intra-tumoral heterogeneity. Current standard therapy includes maximal safe surgical resection, followed by concurrent radiation and/or adjuvant chemotherapy. However, in spite of intensive treatment, patients have a poor prognosis, due to the high recurrence potential of GBM. Identifying GBM biomarkers could help in earlier disease diagnosis, patient classification and stratification, as well as in the characterization of specific features regarding the tumor physiology and aggressiveness, paving the way to new therapeutic strategies.

Growing evidence indicate that GBM exploits mechanisms of neurogenesis and neurodevelopment to further facilitate tumor progression. There is recent evidence suggesting, high expression of the Promyelocytic Leukemia Protein (PML), a tumor suppressor and cell regulator, in primary GBM samples. PML is expressed in all tissues and implicated in various ways to cancer biology. In brain, PML participates in the physiological migration of the neural progenitor cells, which have been also hypothesized to serve as the cell of origin of GBM. Recent studies in PML knocked-down mice indicate a common PML-mediated migratory pathway in both adult neurogenesis and GBM invasion within the central nervous system. Furthermore, recent findings in the biology of malignant gliomas have revealed that glioma cells extend long membranous protrusions called tumor microtubes (TMs), which share certain characteristics with the axonal and dendritic growth of developing neurons. TMs are utilized as pathways for the proliferation and invasion of brain tumors and serve as points of intersection for the formation of the GBM network, enabling rapid and long-distance multicellular communication. Intercellular calcium waves propagate through this network via gap junctions and synchronize GBM cells, orchestrating various cellular activities that promote tumor progression and resistance to therapeutic interventions.

In this work, we aim to explore more thoroughly the role of PML in GBM growth, invasion, glioma network formation, and treatment by utilizing a variety of models including 2D/3D *in vitro* and *ex vivo* cultures. In our experiments, we utilize the established U87MG cell line, which has been genetically modified for conditional overexpression or silencing of the PML protein. Specifically, we explore the role of the PML protein in the proliferation of GBM cells using 2D *in vitro* biological models. Additionally, we examine whether the PML protein can modulate the TM-network and we investigate the effect of TM-network on GBM proliferation and response to treatment by employing the gap junction channel blocker carbenoxolone (CBX). Moving beyond 2D cultures, we employ advanced 3D biological models, such as spheroids and organotypic brain slices (*ex vivo*), to explore the PML-mediated effects on tumor growth and invasion. To visualize and quantify these effects, we utilize conventional optical microscopy techniques along with confocal microscopy.

Our overall findings indicate that PML overexpression suppresses cell proliferation, while it induces the invasive capacity of the U87MG cells. Furthermore, the

organotypic brain slices seemed to facilitate further the invasive capacity of GBM cells and the maintenance of the invasive patterns in both *in vitro* and *ex vivo* conditions affirm the consistency of our observations in a more physiologic realistic environment. Moreover, our findings suggest that the PML protein can influence the connectivity of the GBM network. Finally, our results indicate that GBM network plays a role in tumor growth, as evidenced by the observed effect of inhibiting gap junctions with CBX. Unravelling further the various factors affecting GBM proliferation, invasion and treatment response, as well as the various evolutional trajectories brought on by clonal alterations in gliomas, could pave the way into new therapeutic strategies and the identification of potential biomarkers for GBM progression.

2. ΠΕΡΙΛΗΨΗ

Το Γλοιοβλάστωμα είναι ο πιο κακοήθης καρκίνος του εγκεφάλου μεταξύ των ενηλίκων, σύμφωνα με τον Παγκόσμιο Οργανισμό Υγείας (WHO). Χαρακτηρίζεται από υπέρμετρο πολλαπλασιασμό, διήθηση και υψηλή κυτταρική ετερογένεια. Η τρέχουσα θεραπεία περιλαμβάνει τη μέγιστη ασφαλή χειρουργική αφαίρεση του όγκου, η οποία ακολουθείται από ακτινοθεραπεία και χημειοθεραπεία. Ωστόσο, το προσδόκιμο όριο των ασθενών με Γλοιοβλάστωμα παραμένει πολύ χαμηλό, καθώς υπάρχει υψηλή πιθανότητα υποτροπής. Η ταυτοποίηση βιο-δεικτών του Γλοιοβλαστώματος θα μπορούσε δυνητικά να συμβάλει στην καλύτερη και έγκαιρη διάγνωση της νόσου καθώς και στον προσδιορισμό συγκεκριμένων χαρακτηριστικών της φύσης του όγκου κάθε ασθενούς.

Αυξανόμενα στοιχεία υποδηλώνουν ότι το Γλοιοβλάστωμα εκμεταλλεύεται μηχανισμούς νευρογένεσης και νευροανάπτυξης για να ευνοήσει περαιτέρω την εξέλιξη του. Πρόσφατες μελέτες υποδεικνύουν υψηλή έκφραση της Πρωτεΐνης της Προμυελοκυτταρικής Λευχαιμίας (PML), σε πρωτογενή δείγματα Γλοιοβλαστώματος. Η PML είναι μια ογκοκατασταλτική πρωτεΐνη, η οποία έχει φυσιολογικό ρόλο κυτταρικού ρυθμιστή. Η PML εκφράζεται σε όλους τους ιστούς και σχετίζεται με διάφορους τρόπους με την βιολογία του καρκίνου. Στον εγκέφαλο, η PML συμμετέχει στη φυσιολογική μετανάστευση των νευροβλαστών, οι οποίοι έχουν επίσης υποτεθεί ότι είναι τα κύτταρα προέλευσης του Γλοιοβλαστώματος. Πρόσφατες μελέτες σε ποντίκια στα οποία είχε κατασταλεί η PML έδειξαν ένα κοινό μεταναστευτικό μονοπάτι μεταξύ της ενήλικης νευρογένεσης και της διηθητικότητας του Γλοιοβλαστώματος στο κεντρικό νευρικό σύστημα. Επιπλέον, πρόσφατα ευρήματα στη βιολογία των κακοήθων γλοιωμάτων έχουν αποκαλύψει ότι τα γλοιωματικά κύτταρα εκτείνουν μακριές μεμβρανώδεις προεξοχές, οι οποίες ονομάζονται tumor microtubes (TMs), που μοιράζονται συγγενή χαρακτηριστικά με την αξονική και δενδριτική ανάπτυξη των νέο-αναπτυσσόμενων νευρώνων. Τα TMs χρησιμοποιούνται ως μονοπάτια για τον πολλαπλασιασμό και την διήθηση των όγκων του εγκεφάλου και λειτουργούν ως σημεία διασύνδεσης για το σχηματισμό του γλοιωματικού δικτύου που επιτρέπει τη γρήγορη και μεγάλης απόστασης πολυκυτταρική επικοινωνία. Διακυτταρικά κύματα ασβεστίου διαδίδονται μέσω αυτού του δικτύου μέσω των gap junctions εναρμονίζοντας διάφορες κυτταρικές λειτουργίες που προωθούν την εξέλιξη του όγκου και την αντίσταση στις θεραπευτικές παρεμβάσεις.

Σε αυτήν την εργασία, θα μελετήσουμε πιο εκτενώς και συμπληρωματικά τον ρόλο της PML στην ανάπτυξη, την διήθηση, το σχηματισμό του γλοιωματικού δικτύου και τη θεραπεία του Γλοιοβλαστώματος, χρησιμοποιώντας μια ποικιλία μοντέλων, συμπεριλαμβανομένων 2D/3D καλλιεργειών *in vitro* και μοντέλων *ex vivo*. Στα πειράματά μας, χρησιμοποιείται η εγκαθιδρυμένη κυτταρική σειρά U87MG, στην οποία επιτελείται υπερέκφραση/αποσιώπηση της πρωτεΐνης PML. Συγκεκριμένα, διερευνάται ο ρόλος της πρωτεΐνης PML στον πολλαπλασιασμό των κυττάρων του Γλοιοβλαστώματος χρησιμοποιώντας 2D βιολογικά μοντέλα *in vitro*. Επιπλέον, εξετάζουμε εάν η πρωτεΐνη PML μπορεί να ρυθμίσει το γλοιωματικό δίκτυο και διερευνούμε το αντίκτυπο του δικτύου στο πολλαπλασιασμό του Γλοιοβλαστώματος

και στην ανταπόκριση στη θεραπεία, χρησιμοποιώντας έναν αναστολέα των gap junctions. Εκτός από τις 2D καλλιέργειες , χρησιμοποιούμε προηγμένα 3D βιολογικά μοντέλα, όπως σφαιρίδια και οργανοτυπικές φέτες εγκεφάλου (*ex vivo*), για να εξετάσουμε τις επιδράσεις που μεσολαβούνται από την PML στην ανάπτυξη και την διήθηση του όγκου. Για να οπτικοποιήσουμε και να ποσοτικοποιήσουμε αυτές τις επιδράσεις, χρησιμοποιούμε συμβατικές τεχνικές οπτικής μικροσκοπίας μαζί με συνεστιακή μικροσκοπία.

Τα ευρήματα αυτής της δουλειάς υποδεικνύουν ότι η υπερέκφραση της PML καταστέλλει τον πολλαπλασιασμό , ενώ παράλληλα ευνοεί την διήθηση των γλοιωματικών κυττάρων της σειράς U87MG. Παρόλο που οι οργανοτυπικές φέτες εγκεφάλου διευκολύνουν περαιτέρω την διήθηση των κυττάρων του Γλοιοβλαστώματος , η διατήρηση των μοτίβων διήθησης τόσο στα *in vitro* όσο και στα *ex vivo* επιβεβαιώνει τις παρατηρήσεις μας. Επιπλέον, τα ευρήματά μας υποδηλώνουν ότι η PML επηρεάζει τη συνδεσιμότητα του γλοιοωματικού δικτύου . Τέλος, τα αποτελέσματά μας , δείχνουν ότι το δίκτυο του Γλοιοβλαστώματος παίζει ρόλο στην ανάπτυξη του όγκου, όπως αποδεικνύεται από τον παρατηρούμενο αντίκτυπο της αναστολής των gap junctions με την καρβενοξολόνη (CBX). Η περαιτέρω αποκωδικοποίηση των διαφόρων παραγόντων που επηρεάζουν το πολλαπλασιασμό, την διήθηση και την ανταπόκριση στη θεραπεία του Γλοιοβλαστώματος θα μπορούσε να ανοίξει το δρόμο για νέες θεραπευτικές στρατηγικές και δυνητικούς βιο-δείκτες για την εξέλιξη της νόσου.

3. INTRODUCTION

3.1. Glioblastoma (GBM)

Glioblastoma Multiforme (GBM) is a highly aggressive and malignant type of brain cancer that is classified as grade IV according to the World Health Organization (Louis et al., 2016). GBMs are associated with a poor prognosis despite multimodal treatment due to their extensive heterogeneity, complex biology, invasive nature, and colonization of the entire brain. GBM cells invade the neighboring brain parenchyma and expand further from the tumor bulk to the periphery, forming the brain tumor lesion and making GBM a diffusive rather than a focal disease. The majority of glioblastoma cases, approximately 90% are classified as primary glioblastomas and occur *de novo*, primarily affecting older patients with no indication of a less malignant precursor lesion. In contrast, 10 % of the cases are classified as secondary glioblastomas, which are characterized by a history of prior lower grade diffuse glioma, which preferentially affect younger patients (Ohgaki & Kleihues, 2013).

Glioblastomas comprise 46.1% of all malignant primary brain tumors. Incidence of glioblastoma increases with age, with a median age of diagnosis at 64 years. The median survival post-diagnosis for GBM is 14 months with less than 5% of patients surviving more than 5 years (Ostrom et al., 2014). Survival outcomes are known to decline with increasing age (Wirsching & Weller, 2017).The current treatment for newly diagnosed glioblastoma is consisting of maximum safe resection followed by fractionated localized radiotherapy and maintenance chemotherapy (Stupp et al., 2005). Despite these efforts, the prognosis of GBM remains poor.

3.1.a. GBM origin

The brain consists of hundreds of different cell types resulting to the question of the origin of GBMs. Tumor cells with stem cell characteristics, known as cancer stem cells (CSCs) were successfully isolated from human gliomas, implies that neural stem cells (NSCs) may be the source of origin (Singh et al., 2004). A few other studies using genetic mouse models provided some supportive evidence for this hypothesis (Zheng et al., 2008; Zhu et al., 2005). In other studies oligodendrocyte precursor cells (OPCs) - a glial cell progenitor - act as cell of origin for human gliomas or the proneural subtype of GBM (Lei et al., 2011a; Liu et al., 2011). OPCs, reflected by their name, were originally believed to function solely as the precursor for mature oligodendrocytes. However, the possible role for OPCs as the glioma origin has been further supported by other studies (Lei et al., 2011b).

3.1.b. GBM heterogeneity and microenvironment

The extensive diversity in genetic and phenotypic makeup among GBM cells within a single tumor (intra-tumoral heterogeneity) and between different GBM patients (inter-tumoral heterogeneity), along with the dynamic interplay of various sub-populations coexisting within a tumor, limits progress in implementing novel, effective treatment protocols. GBMs are composed of a highly heterogeneous mixture of cells that exhibit varying degrees of cellular and nuclear polymorphism (Soeda et al., 2015). This heterogeneity can be observed not only between patients but also within a single tumor. This heterogeneity can include different cell populations or clones which may have distinct morphologies, levels of differentiation, genetic mutations and gene expression profiles (McLendon et al., 2008). Moreover, various histological phenotypes can be seen such as small cell glioblastoma, glioblastoma with a primitive neuronal component, oligodendroglioma-like components, or giant cell glioblastoma (Perrin et al., 2019). This complex and diverse nature of glioblastomas greatly complicates efforts to understand and combat the disease.

Instead of focusing on cell-intrinsic pathways, many research studies are now intervene by manipulating the extracellular environment and the interactions of tumor cells with this environment, which is known to play a crucial role on tumor progression. The tumor microenvironment (TME), refers to the non-cancerous cells and biomolecules that exist within a tumor and support its growth. These cells include normal and reactive astrocytes, glioblastoma stem cells (GSCs), fibroblasts, immune cells, microglia/macrophages, endothelial cells (ECs), vascular pericytes, and neurons. Recent findings have demonstrated that glioma cells form bona-fide glutamatergic excitatory synapses with neurons (Venkataramani et al., 2019; Venkatesh et al., 2015). Furthermore, GBM cells are also functionally connected to astrocytic networks. The TME also consists of biomolecules within the tumor, and the extracellular matrix (ECM). Noncancerous cells produce various biomolecules, including cytokines, chemokines, hormones, and nitric oxide (NO). GBM microenvironment also includes glycosaminoglycans (GAGs) proteins (Schiffer, 2018). GAGs play a crucial role in interacting with proteins such as proteases, growth factors, cytokines, chemokines, and adhesion molecules, facilitating physiological processes like protein function, cellular adhesion, and signaling.

3.1.c. GBM migration, invasion, infiltration

The migration and invasion of GBM cells is a highly complex process, that is regulated by multiple factors, including changes within the migrating cells as well as the TME. GBM cells can migrate into the neighboring brain parenchyma and expand, characterizing GBM as a highly diffusive disease (Claes et al., 2007). Specifically, glioma cells migrate along existing brain structures such as the brain parenchyma, blood vessels, white matter tracts and subpial spaces. These patterns have been described first by Hans Joachim Scherer in 1938 and referred to as “secondary structures of Scherer” (Scherer, 1938). These distinctive morphological patterns play a crucial role in understanding the invasive nature of GBM cells and their interaction with the

surrounding brain environment. Invadopodia are a functional cellular structure that is critical for the invasion of glioblastoma. These structures enable cancer cells to migrate and invade by actin polymerization, integrin signaling and degrading the surrounding ECM through matrix metalloproteinase secretion (Mallawaaratchy, 2015). Moreover, tumor invasion and recurrence have been long associated with the processes of angiogenesis and vasculogenesis (Angara et al., 2017). Hence the development of novel approach to manage the local invasion of these infiltrating cells holds significant promise for the successful eradication of these tumors.

3.1.d. Tumor Microtubes (TMs) in GBM and the role of TM network in proliferation, invasion and resistance

Glioma cells exhibit extensive membranous extensions recognized as tumor microtubes (TMs). TMs are highly dynamic structures used for scanning the brain invasion and are responsible for the establishment of a resilient malignant tumor-tumor cell network resistant to therapeutic interventions (Osswald et al., 2015). The interconnection of TMs is facilitated by gap junctions, mediated either through connexin 43 or adherens junctions (Schneider et al., 2021). Using gap junctions, the tumor cells can exchange small molecules such as calcium ions, ATP, IP3, and microRNA (Osswald et al., 2015).

This tumor network contributes to glioma progression and resistance to all standard of care treatments including surgery, radiation, and chemotherapy. Notably, TMs exhibit a remarkable capacity to extend towards the site of a surgical lesion and to recolonize the injury site. This phenomenon illustrates the self-repairing mechanisms of this malignant network and its contribution to therapeutic resistance after surgery (Weil et al., 2017). Other studies have revealed that the subpopulation of brain-colonizing glioblastoma cells is strongly enriched for stem-like cellular features (Xie et al., 2021). Further analysis of human gliomas revealed that TMs formation was highly influenced by tumor type and grade, with a marked positive correlation between TMs length and unfavorable prognosis (Osswald et al., 2015).

Increasing evidence emerges showing how neurodevelopmental mechanisms and the nervous system play a pivotal role in brain tumor initiation and progression. Specifically, dynamic TMs at the invasive front share similarities with axonal growth cones and neurite outgrowth during neurodevelopment. Studies examining the impact of neuronal activity on glioma cell proliferation in patient-derived xenograft models uncovered a notable rise in the tumor cell proliferation (Venkatesh et al., 2015). Apart from the gap junction-coupled tumor network, bona fide glutamatergic synapses formed between neurons and glioma cells were found in tumor subpopulations of adult isocitrate dehydrogenase wildtype (IDH-wt) glioblastomas and adult isocitrate dehydrogenase mutant (IDH-mut) astrocytoma (Venkataramani et al., 2019). In addition to synaptic communication, paracrine signaling represents a crucial aspect of neuron-glioma interaction. Within the tumor microenvironment, paracrine factors are released, exerting influence on the progression of the tumor by fostering the growth and proliferation of high-grade gliomas (Venkatesh et al., 2019).

In summary, neuron-glioma synapses mediate proliferation, invasion, and TMs generation and dynamics. All this evidence, suggests a reciprocal interaction between neurons and glioma cells, potentially giving rise to a positive feedback loop and subsequent establishment of a vicious cycle (Yang et al., 2022). Furthermore, TMs have been identified to fulfill two fundamental biological roles: firstly, serving as leading structures facilitating the invasion and proliferation of glioma cells, thereby enabling efficient brain colonization; and secondly, acting as conduits that interconnect individual glioma cells into a cohesive syncytium. This network formation leads to the establishment of a functional and resistant network within the glioma microenvironment (Osswald et al., 2016; Weil et al., 2017).

3.1.e. Diagnosis and treatment of GBM

Glioblastomas are typically diagnosed upon symptomatic presentation, arising from their rapid growth and invasive impact on brain structures. Indicative symptoms may include newly manifested epilepsy, headaches, focal neurological signs, and alterations in mental status, in combination with increased intracranial pressure (Weller et al., 2014). Following maximal safe resection, the generally accepted treatment for glioblastoma is radiotherapy with concurrent temozolomide (TMZ) chemotherapy.

- ***Antitumor efficacy of TMZ***

The most common chemotherapy drug used for glioblastoma is the blood–brain barrier-permeable drug TMZ and is applied in the clinic since 2005 as the gold-standard treatment for most brain tumors, including GBMs. Moreover, TMZ has shown effective antitumor activity in various human xenografts, including melanoma, ovarian, and colon tumors (Stupp et al., n.d.). TMZ is a second-generation alkylating chemotherapy agent, belonging to the imidazole derivative class and it is known to induce cell cycle arrest at G2/M and to eventually lead to apoptosis. At a PH greater than 7, TMZ undergoes spontaneous hydrolysis to form the active metabolite 5-(3-methyl)-1-triazen-1-yl-imidazole-4-carboximide (MTIC). MTIC is further hydrolyzed to 5-amino-imidazole-4-carboxamide (AIC) and to methylhydrazine. The cytotoxicity of TMZ is mediated by the addition of methyl groups at N7 and O6 sites on guanines, as well as the O3 site on adenines, leading to alkylation in genomic DNA. Alkylation of the O6 site on guanine induces the insertion of a thymine instead of a cytosine during subsequent DNA replication, ultimately resulting in cell death (*Fig.1*) (Chelliah et al., 2021; Lee, 2016).

The therapeutic success of TMZ is assumed to depend on the absence of the methylguanine-DNA methyltransferase (MGMT). MGMT is a repair enzyme that removes the methyl group from the O6-position of guanine, thereby preventing further mismatches (Lee, 2016). High levels of MGMT activity in cancer cells contribute to a resistant phenotype by diminishing the effectiveness of alkylating agents. This increased MGMT activity is a significant factor that can lead to treatment failure. Most tumor cells are innately resistant to TMZ at pharmacotherapeutic doses or quickly develop resistance (Lee, 2016). The clinical use of TMZ is, however, limited by its general toxicity, as it

modifies the DNA of all cells in an indiscriminate manner. Severe cases of hematological toxicity as well as hepatotoxicity have been described (Stepanović et al., 2018). Other findings suggest that autophagy is a main part of TMZ-induced cytotoxicity and that inhibition of the autophagic process significantly influences the antitumor effect of TMZ (Kanzawa et al., 2004).

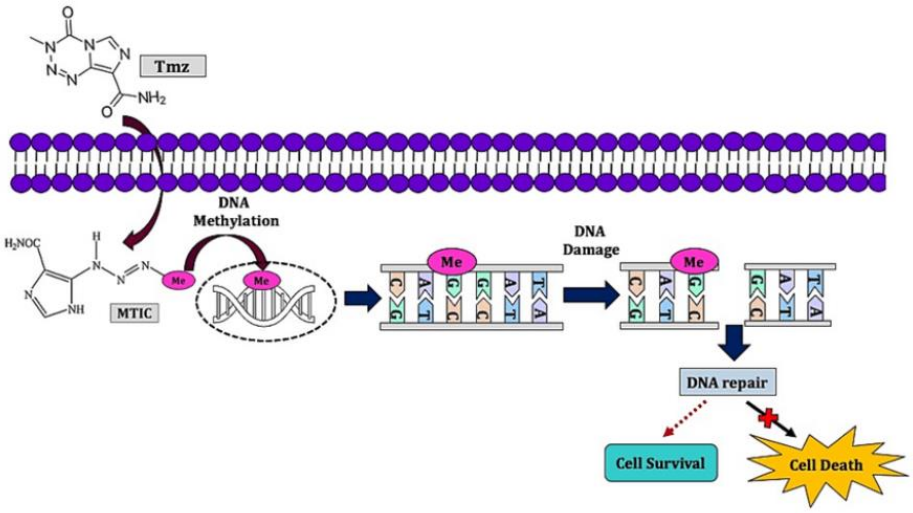

Figure 1. Schematic depiction of TMZ mode of action. TMZ undergoes spontaneous hydrolysis intracellularly to form monomethyl triazene 5-(3-methyltriazen-1-yl)-imidazole-4-carboxamide (MTIC). MTIC then hydrolyzed to form 5-aminoimidazole-4-carboxamide, which later converts into methylhydrazine. Methyldiazonium, an active cation, then methylates the nucleobases, preferentially N 7 position of guanine (N 7 -MeG; 70%), guanine rich site and to a certain extend at N 3 adenine (N 3 -MeA; 9%) and O 6 guanine residues (O 6 -MeG; 6%) (Chelliah et al., 2021;)

- ***In vitro studies of TMZ***

GBM cell lines have been widely used to study the biology of GBM and to test therapeutic approaches, including elucidating the effects of TMZ. Studies using *in vitro* models of glioma cells exhibited a tendency toward reduced growth and notable alterations in cell morphology following prolonged exposure to TMZ (Wu et al., 2019). These observations imply potential modifications in cell cycle dynamics and the regulation of the cellular cytoskeleton. The time and dose-dependent effects of TMZ on cell growth and viability of the U87-cell line have been examined as well. A TMZ dose-related decrease in cell viability has been noted at a TMZ concentration of 200 μM. However, TMZ sensitivity varies between cell line. TMZ inhibited the cell viability of all tumor cells in a dose-dependent manner (Fisher et al., 2007). Other studies explore the synergistic effects of combining TMZ with other anticancer agents or treatment modalities in the U87 cell line, aiming to enhance therapeutic outcomes. Combination therapy, utilizing multiple anticancer agents, has garnered increased

attention as a viable strategy to combat drug resistance in cancer treatment. This approach not only facilitates a reduction in both dosage and associated side effects but also serves to forestall or impede the development of drug resistance (Khaz, n.d.; Pazhouhi et al., n.d.).

- ***GBM network and TMZ***

Resistance of glioblastoma to the front-line chemotherapeutic agent TMZ continues to challenge GBM treatment efforts. Network integration increases glioblastoma cell resilience by improved cellular homeostasis, like that of intracellular calcium(Osswald et al., 2015). Consequently, disturbance of the ability of glioblastoma cells to integrate in TM-connected networks makes radiotherapy and TMZ chemotherapy more effective. Network disconnection can be achieved pharmacologically or genetically (Winkler, 2021). Recent studies indicate that the gap junction protein connexin 43 (Cx43) renders GBM cells resistant to TMZ through its carboxyl terminus (CT) (Murphy et al., 2016). Current available studies on pharmacological gap junction inhibition in glioblastoma are mainly based on the use of the glycyrrhetinic acid-derivative carbenoxolone as a potent gap junction blocker (Yulyana et al., 2013). In terms of glioblastoma biology pharmacological gap junction inhibition by carbenoxolone yielded additive effects on survival rates in temozolomide-treated orthotopic xenograft models in mice (Hitomi et al., 2015).

Taken together, these data demonstrate the anti-tumor effect of gap junction inhibition in pre-clinical GBM models and suggest increased efficacy when combined with TMZ. These findings suggest that gap junction inhibitors can be used to override the development of TMZ resistance and potentially that of other chemotherapy drugs as well (Hitomi et al., 2015).

3.2. Promyelocytic leukemia protein (PML)

3.2.a. PML characteristics

The PML gene was first identified through chromosomal translocation with the retinoic acid receptor alpha (RARa), which accounts for 99% of all cases of acute promyelocytic leukemia (APL). The t (15;17) translocation results in the formation of two reciprocal fusion products: PML/ RARa and RARa/PML(Alcalay et al., 1991; Borrow et al., 1990; de Thé et al., 1991; Ruggero et al., 2000). PML is implicated in the control of several cellular processes.

3.2.b. PML structure

The PML gene encompasses nine predominant exons, resulting in the production of a diversity of PML isoforms through alternative splicing. These isoforms are divided into seven groups, PML I to VII, which all have a common N-terminal region but differ in their C-terminal sequences (*Fig.2*)(de Thé et al., 1991; Jensen et al., 2001). All the isoforms of PML protein's functional domains collectively form the RBCC motif or TRIpartite MOtif (TRIM) at their N-terminus, including a zinc-binding domain with a RING finger and two cysteine/histidine-rich B-boxes (B1 and B2) and a coiled-coil helical domain (Jensen et al., 2001). The RBCC domain not only regulates PML's ability to form dimers and multimeric complexes but also its interaction with several proteins (Previati et al., 2018; Ruggero et al., 2000).

The presence of a nuclear localization signal (NLS) within the PML protein has been observed and its deletion has been demonstrated to result in a distinct cytoplasmic and perinuclear localization pattern (Le et al., 1996). In fact, there are six nuclear PML isoforms designated PMLI to PML VI and one cytoplasmic isoform PMLVII (Jensen et al., 2001). The isoforms are numbered based on their size with PMLI being the longest one and PMLIVII the shortest one. In addition to the seven primary isoforms, other possible isoforms may exist due to potential alternative splicing of exons 4, 5 and 6. The different C-termini parts among the PML isoforms may indicate isoform-specific actions (Nisole et al., 2013a).

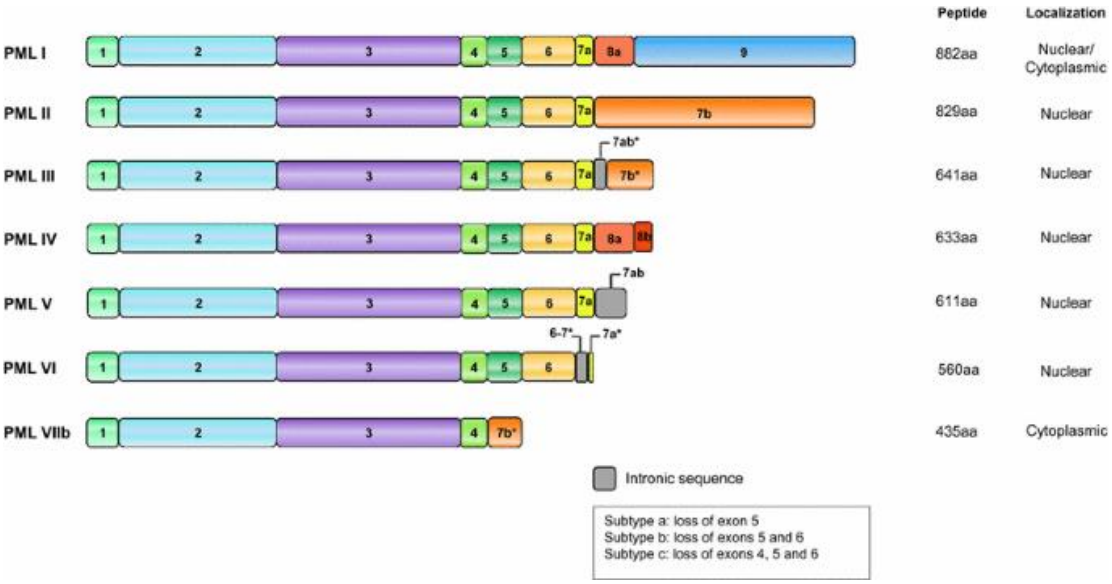

Figure 2. Schematic of PML isoforms and their localizations. The primary PML transcript is organized into 9 exons and can be alternatively spliced to generate up to seven known class of isoforms that share exons 1–4.

3.2.c. Subcellular distribution of PML

PML expression has been identified in two distinct subcellular compartments within the nucleus: the diffuse fraction of the nucleoplasm and a discrete subnuclear entity known as nuclear bodies (NBs). This subnuclear structure has been referred to by various nomenclatures including ND10 (Nuclear Domain 10), Kremer (Kr) Bodies (Ascoli & Maul, 1991; Ruggero et al., 2000). It is typical for cells to harbor 5 to 30 nuclear bodies (NBs) per nucleus, which exhibit diameters ranging from 0.1 to 1mm (Bernardi & Pandolfi, 2007). However, the number and size fluctuate throughout the cell cycle and the cell type (Bernardi & Pandolfi, 2007; Lallemand-Breitenbach & de Thé, 2010; Ruggero et al., 2000).

These structures are primary composed of proteins and lack DNA or RNA(Lallemand-Breitenbach & de Thé, 2010). The primary structural component of the PML Nuclear Body (NB) is the PML protein, which primarily constitutes the outer shell of the bodies (Lallemand-Breitenbach & de Thé, 2010). The PML Nuclear Bodies (NBs) have been implicated in a wide range of biological processes including gene transcription, both activation and repression, viral pathogenicity (Zhong, 2000), tumor suppression, proteasomal degradation, cellular senescence, apoptosis and DNA repair (Seeler, 1999), (Dellaire, 2004), stem cell maintenance, but their overall biochemical function is not yet clearly defined (Lallemand-Breitenbach V. a., 2018).

3.2.d. PML in brain

PML is found in neurons and plays a role in various aspects of the nervous system, such as the development of the brain, regulation of circadian rhythms, plasticity and response to proteins that cause neurodegenerative disorders (Korb, 2013). More specifically, researchers found that PML protein is abundant in germinal regions in the developing brain and that the absence of PML leads to an increase in the number of proliferating NPCs (Regad, 2009). More specifically, in the brain, PML has been shown to participate in the forebrain development(Regad et al., 2009). It has been found that PML expression is limited to the Neural Progenitor/Stem Cells (NPCs) in the developing mouse cortex (Regad et al., 2009)and it regulates the NPC physiological migration from the Sub-Ventricular Zone (SVZ) to the Olfactory Bulb (OB) through the Rostral Migratory Stream (RMS) (Amodeo et al., 2017). This NPC migration is achieved via a PML-mediated suppression of Slits (Amodeo et al., 2017) which are fundamental components in brain circuits development and axon guidance especially during SVZ neurogenesis. PML controls the PML/Slit axis via the Polycomb repressive complex 2 (PRC2) (Amodeo et al., 2017).

Expression of PML has also been reported in supraoptic neurons of the normal adult human brain (Villagra, 2006). In addition, it has been reported that PML protein is completely or partially lost in a large fraction of human cancers and that loss of PML protein correlates with tumor progression (Gurrieri, 2004). Despite the widespread acceptance of PML as a tumor suppressor among the scientific community, there remain a few exceptions. Many researchers suggest that PML can have both tumor -

promoting or tumor-inhibiting effects regarding the type or the tissue origin of the tumor (Mazza, 2013). Another study has been shown that PML can inhibits tumor growth but the tumor cells maintain their migratory capacity (Tampakaki et al., 2021). The pleiotropic functions of PML in tumor suppression suggest that inactivation or downregulation of PML would provide an advantage for tumor development and progression. Although the evidence is growing, there is still no cohesive view on the function of PML in the adult brain. One possibility is that PML protein has multiple roles, which vary between regions or physiological context.

3.3 Culture models for GBM research

At present, several research models are helping researchers understand the biological mechanisms of GBM. Traditional *in vitro* cell cultures have provided valuable insights into basic molecular and cellular mechanisms, offering a controlled environment for studying specific aspects of glioblastoma biology. Additionally, xenograft models, where human glioblastoma cells are transplanted into immunodeficient mice, enable the investigation of tumor growth and response to therapies within an in vivo setting. Genetically engineered mouse models (GEMMs) have been pivotal in elucidating the complex genetic alterations associated with glioblastoma initiation and progression. Patient-derived xenografts (PDX) involve implanting human glioblastoma tissue directly into mice, preserving the unique characteristics of individual tumors and facilitating personalized medicine approaches. Furthermore, organotypic slice cultures provide a bridge between in vitro and in vivo models, allowing researchers to explore glioblastoma behavior in a setting that maintains some aspects of tissue architecture and microenvironment. Each of these models contributes distinct advantages, collectively enhancing our comprehension of glioblastoma pathobiology and aiding in the development of novel therapeutic strategies.

3.3.a. Cell lines

In order to study the GBM tumor pathophysiology and identify specific molecular and cellular mechanisms contributing to oncogenesis or tumor maintenance, a variety of biological models have been applied in GBM research (Grotzer et al., 2016; Klinghammer et al., 2017; Oraiopoulou et al., 2018). Currently, there are plenty of established GBM cell lines reported in bibliography, assigned to the vast majority of GBM molecular subtypes. Yet, they often fail to reliably predict the clinical response. The evolutionary process that tumors undergo during clonal selection can only be approached with biological models that maintain the intrinsic tumoral heterogeneity (Klinghammer et al., 2017; Oraiopoulou et al., 2018). Therefore, the latest trends in GBM research employ patient-derived, primary cell lines, that better resemble the heterogeneous nature and the complexity of the disease, and they are closer to the original tumor (Oraiopoulou et al., 2017).

Secondary cell lines, on the other hand, have been extensively used in GBM research since they are well profiled, easily manipulated (Klinghammer et al., 2017) and suitable to study specific cellular mechanisms (Klinghammer et al., 2017; Oraiopoulou et al., 2017). They can also serve as controls for patient-derived cells (Oraiopoulou et al., 2017) and as a common ground across diverse studies. U87MGClick or tap here to enter text.and T98G (Stein, 1979) (Matsumura et al., 2000) are two well-known GBM secondary cell lines, which are representative of most common GBM proliferative and invasive phenotypes and therefore often used in GBM experimental models. Especially the T98G cell line is highly representative of the GBM invasive behavior in vitro, ex vivo and in vivo studies, due to cell-to-cell/matrix adhesion, epithelial-to-mesenchymal transition (EMT) and metabolic and microenvironmental factors (Adamski et al., 2017). All secondary lines tend to differ from the tumor of origin due to clonal selection, hence they are characterized by less phenotypic heterogeneity and higher level of differentiation than the primary cell lines (Allen et al., 2016). Nonetheless, both the U87MG and the T98G cell lines are well-characterized and widely accepted as valid GBM experimental models (Allen et al., 2016; Kiseleva et al., 2018).

3.3.b. Three-dimensional (3D) in vitro models

Biological 3D models (i.e., spheroids) that describe the early phases of tumor development in a tissue context more accurately can serve as intermediate systems between traditional 2D cell culture and complex *in vivo* models. The limited cell–cell interactions in 2D monolayer cultures introduce major changes in cellular physiology. Tumor spheroids comprise a well-characterized model system, which is able to reproduce the spatial organization and micro-environmental factors of *in vivo* micro tumors, i.e., the relevant gradients of nutrients and other molecular agents, as well as the deposition of ECM. Primary GBM cells growing into tumor spheroids in a similar specialized medium and studied under different environmental conditions comprise an important first step for exploring GBM bio-complexity. Therefore, 3D cultures of the same cells may represent the original organ or tumor more faithfully than traditional cell cultures (Humpel, 2015).

The behavior and potential fate of every human cell are influenced by its immersion in a three-dimensional microenvironment. Consequently, in vitro models employed to investigate glioma biology and develop efficacious therapies ought to replicate the TME as closely as possible. Through primary in vitro cells cultures, researchers can examine various aspects such as cell survival, morphology, function, as well as the effects of toxic and protective substances.

- ***Spherical cancer models***

Spherical cancer models are characterized by the presence of sphere -like structures primarily or entirely composed of cancer cells. These models are widely used in 3D in vitro studies due to their ease of production. A classification for spherical models has been proposed by Weiswald et al (Weiswald et al., 2015), delineating four main types

with their respective features and culture conditions : 1) multicellular tumor spheroids, which are produced under non-adherent conditions from single -cell suspensions; 2) tumorospheres, which serve as models for the culture and expansion of CSCs; 3) tissue-derived tumor spheres, exclusively composed of cancer cells following partial dissociation of cancer tissues; and 4) organotypic multicellular spheroids, generated by sectioning cancer tissue under non adherent conditions (Weiswald et al., 2015).

Among these types, tumorspheres, represent one of the key spherical cancer models. Tumorspheres, are formed by the proliferation of single- cell suspensions derived from tissue, circulating cancer cells, or established cell lines (resulting from clonal expansion). Tumorspheres possess the capability to maintain the multipotency of CSCs and exhibit 3D interactions that resemble the oxygen and nutrient gradient within tumors. Consequently, tumorspheres display a quiescent necrotic core surrounded by a more proliferative outer layer (Ruiz-Garcia et al., 2020). Tumor spheres can be grown in suspension in the regular specific cell media or submerged in a gel.

Multicellular tumor spheroids (MCTSs), commonly known as glioma tumor spheroids, represent another type of spherical cancer model. Different culture methods and techniques have been developed to facilitate a large number of cells under non -adherent conditions and promoting their aggregation and compaction. Typically, established cell lines are cultured using serum -supplemented medium (Oraiopoulou et al., 2019) without the addition of an exogenous ECM. The core principle of the technique is that by creating conditions where the adhesive forces between cells surpass those between the cells and the substrate they are plated on, tumor cells are discouraged from adhering to the underlying tissue culture plastic. Instead, this promotes cell -to cell adhesion, leading to the formation of well-rounded spherical structures. The formation varies depending on the specific cell line and experimental system, typically ranging from 1 to 7 days of culture (Weiswald et al., 2015). Spheroids can be generated by directly seeding cells in ultra-low attachment plates without any coating, as the polystyrene surface of these plates exhibits low-adhesion properties. Another method, the “hanging drop method,” has been described (Weiswald et al., 2015).

- ***Organotypic brain slices***

Over the last decades, organotypic cultures have become a valuable method for replicating in vivo conditions. This approach creates a model system where tumor cells exist within their native microenvironment, as opposed to artificial matrices. Notably, organotypic brain slice cultures exhibit the preservation of essential features including normal cytoarchitecture with cortical lamination and well-preserved pyramidal cells. Moreover, the biochemical and electrophysiological characteristics of neurons are generally sustained over extended periods, exceeding one month(Ohnishi et al., 1998). The extended survival period is attained through the cultivation of slices at an air/liquid interface, achieved either by the continuous rotation of the preparation, as observed in roller-tube cultures (Gähwiler, 1981), or by their cultivation on semiporous membranes in stationary interface cultures (Stoppini et al., 1991).

Brain slices are acquired through precision slicing of tissue using specifically designed machines; the Krum-dieck tissue slicer was considered the golden standard, until more recently the vibrating blade microtome (vibratome) was introduced. Tissue slicing does not interfere with morphology and functional activity of the tissue. Tumor slicing is usually achieved within hours of surgical resection of the primary tumor to minimize deterioration of the tissue and loss of cellular viability(Naipal et al., 2014). Tissue slices can be cultured on membrane inserts with 0.4-μm pores. These inserts position the tissue slice at the air/liquid interface, facilitating effective oxygenation. However, organotypic tissue slice cultures as a model system for studying the brain face a significant drawback in the form of hypoxia. The absence of intact vascularity in tissue slices limits the availability of oxygen to gas diffusion. Various factors, including slice thickness, matrix stiffness, cellularity, and the metabolic and proliferative activity of tumor and stromal cells, influence the extent of oxygen diffusion (Hammond et al., 2014).

Organotypic brain slices offer a valuable approach for investigating diverse aspects of neuronal development and function, including the formation of neuronal networks, synaptic plasticity, electrophysiology, axonal transport, chronic toxicology, gene function, and the migration of neuronal precursors. These organotypic cultures have also been presented as a novel tool to examine the invasive behavior of ex vivo implanted tumor cells.

The invasion of glioblastoma is a highly complex process involving the detachment of tumor cells from the primary tumor site, the formation of new connections with nearby structures, the degradation and/or remodeling of the extracellular matrix, and the dispersion into the surrounding normal brain tissue(Giese et al., 2003). One way to study invasion is by the transplantation of GBM cells into these organotypic brain slices. Studies have been shown that the implanted tumors into the parenchyma of organotypic brain slices strongly resembled the in vivo invasion dynamics of each tumor source and all types of implanted glioma cells invaded strongly into the surrounding tissue (Eisemann et al., 2018; Fayzullin et al., 2016).Specifically, the invasion of GBM cells into the brain slices have been tested with both ways: By grafting tumor spheres or by implanted a cell suspension. Interestingly, only cells from the tumorsphere transplants showed directed invasive movement into the brain parenchyma. The cells in the suspension grafts moved chaotically, and only very few of them left the transplantation zone (Fayzullin et al., 2016).

In conclusion, organotypic tissue slices serve as a solid model system for conducting functional assays. This is attributed to their fast generation time and reflection of intratumor heterogeneity and interactions between tumors and the surrounding stroma. Nonetheless, the existence of various cultivation methods for organotypic tissue slices necessitates the identification of an optimal system.

4. AIM OF STUDY

In this work, we focus on the genetic modifications of the PML protein, in order to unravel its role on GBM cell migration, proliferation and network modulation. The U87MG-GBM cell line was genetically modified with respect to the expression of the PML IV protein, which was either knocked down (U87MG-shPML) or conditionally overexpressed (U87MG-PML OE). PML IV is the most well-studied isoform and it has been previously identified as a strong growth suppressor in various systems (Ivanschitz et al., 2015; Nisole et al., 2013b; Sachini et al., 2019). However, the role of PML IV in the pathophysiology of GBM regarding both the proliferative and infiltrative nature of the disease is still not clear. Specifically, we aim to explore the role of the PML protein in the proliferation of GBM cells using 2D *in vitro* biological models. Additionally, we assess the involvement of the PML protein in the TM-network formation using 2D *in vitro* models, exploring the consequences of altering PML protein levels. Furthermore, we examine the PML-mediated effects on GBM tumor growth and invasive properties by employing advanced 3D biological models, including 3D spheroids and organotypic brain slices. These models will allow for a comprehensive assessment of the influence of the PML protein on the spatial organization and invasive behavior of the GBM cells. Moreover, we seek to investigate further the impact of the TM-network on GBM cell proliferation and treatment response through the utilization of the gap junction (GJ) channel blocker, carbenoxolone (CBX), in established 2D cell culture systems. A preliminary study combining treatment with Temozolomide (TMZ) and CBX is also conducted, in order to identify whether inhibition of GJs and thus, network functionality, affects the response of cells to standard treatment. By further elucidating the effect of the TM-network on GBM cell behavior, our aim is to gain insights into potential therapeutic strategies targeting this network.

5. METHODS

5.1. Cell lines

The well-established human GBM cell lines U87MG (ATCC® HTB-14™) was used in this work. The cells were cultured in Dulbecco's modified Eagle medium (DMEM; Gibco, UK) supplemented with 10% heat-inactivated fetal bovine serum (FBS) and 1‰ gentamycin (PANREAC Applichem, Germany; a.k.a. DMEM^{++}) and incubated in standard lab conditions (37 °C, 5% CO_2).

Generation of the PML-modified Cell Lines. The cells were lentivirusly transfected with an rtTA expressing plasmid (pLenti CMV rtTA3 Blast (w756-1) was a generous gift from Eric Campeau (Addgene plasmid # 26429; http://n2t.net/addgene:26429; RRID: Addgene_26429)). After blasticidin selection, they were further lentivirusly transfected with a plasmid carrying the PML isoform IV, C-terminally fused to the DsRed monomer (Clontech, Mountain View, CA, USA) fluorescent protein (cloned between Xbal and BamHI in PMA2780 (pMA2780 was a gift from Mikhail Alexeyev (Addgene plasmid # 25438; http://n2t.net/addgene:25438; RRID: Addgene_25438) (Alexeyev et al., 2010)). PML expression was controlled by the TET operator and induced upon activation of rtTA by the antibiotic doxycycline (DOXY). In order to induce the PML expression (U87MG-PML OE), DOXY was present in the culture medium at final concentration 0.001ug/ml over time. The presence of the PML protein is visualized by the DsRed fluorophore illumination and the signal is dotted due to the PML-NBs formation within the cell nucleus. Furthermore, to generate the PML knockdown (U87MG-shPML) clone, a lentivirus plasmid pLKO-shRNA against human PML was used. The anti-PML short interfering RNA sequence is 5'-AGATGCAGCTGTATCCAAG-3'. The U87MG-PML transfected cells in the absence of DOXY (non-induced), along with the wild type non-transfected U87MG (U87MG-wt) cell line, served as controls.

5.1.a. 2D *in vitro* cell cultures

- ***Cell proliferation and viability***

Trypan Blue Exclusion. In order to determine the period of time required for the cell lines to double in size and proliferate and their spontaneous cell death occurrence, a protocol adopted by Crowley et al., 2016 was performed. A single cell suspension of 1ml with cell density 20000 cells/ml of culture medium was seeded per well in a 24-well plate at day zero and the plate was incubated in standard lab conditions for 7 days. Every 24h after seeding, the culture medium of one well per cell type was removed and a single cell suspension was produced using trypsin-EDTA (Sigma-Aldrich, Germany) 1X solution. Followingly, the suspension of each cell type is added to 0.4% w/v trypan blue solution of equal volume. The basic principle of trypan blue staining relies on the fact that live cells have intact plasma membranes that can exclude various chemicals,

including trypan blue. Dead or dying cells have ruptured plasma membranes, regardless of the mechanism of death, and therefore cannot exclude trypan blue and appear dark blue in brightfield (Srober, 2015). Thus, the cell concentration of each cell type was measured with a 24h interval using a hemocytometer and the spontaneous cell death percentage was estimated. The proliferation time of each cell line was estimated by applying an exponential linear regression model on the daily cell population data. The spontaneous cell death percentage was estimated as the average percentage of the dead cells compared to the whole cell population.

- ***TMZ and CBX Treatment protocol***

In order to assess the sensitivity of cells to TMZ, concentrations of 500 μM and 1000 μM were used. CBX was administered at following concentrations: (50, 75, 100, 130, 160, 200, 300, 500) μM in order to identify the optimal concentration that inhibits cell growth without causing cytotoxicity. TMZ was also administered in conjunction with an optimal CBX concentration. This combination was added to a 24-well plate on day one, followed by a 7-day incubation in standard lab conditions, following the trypan blue exclusion protocol. The proliferation time and the percentage of spontaneous cell death of each cell line were estimated.

- ***Tumor Microtubes (TMs) Analysis***

Brightfield images were acquired daily up to day 3 employing a 20x magnification to visualize tumor cell interconnectivity and tumor microtube (TMs) branches from 2D cell cultures for all the cell lines. Analysis of images was performed with the software ImageJ (National Institutes of Health). Cells were counted manually. Specifically, soma diameter, TMs total, TMs connected, TMs unconnected, average length of connected and unconnected were estimated. When a TM started at one cell and ended at another, these cells were defined as connected. TMs were counted as shown in the figure below (*Fig.3*).

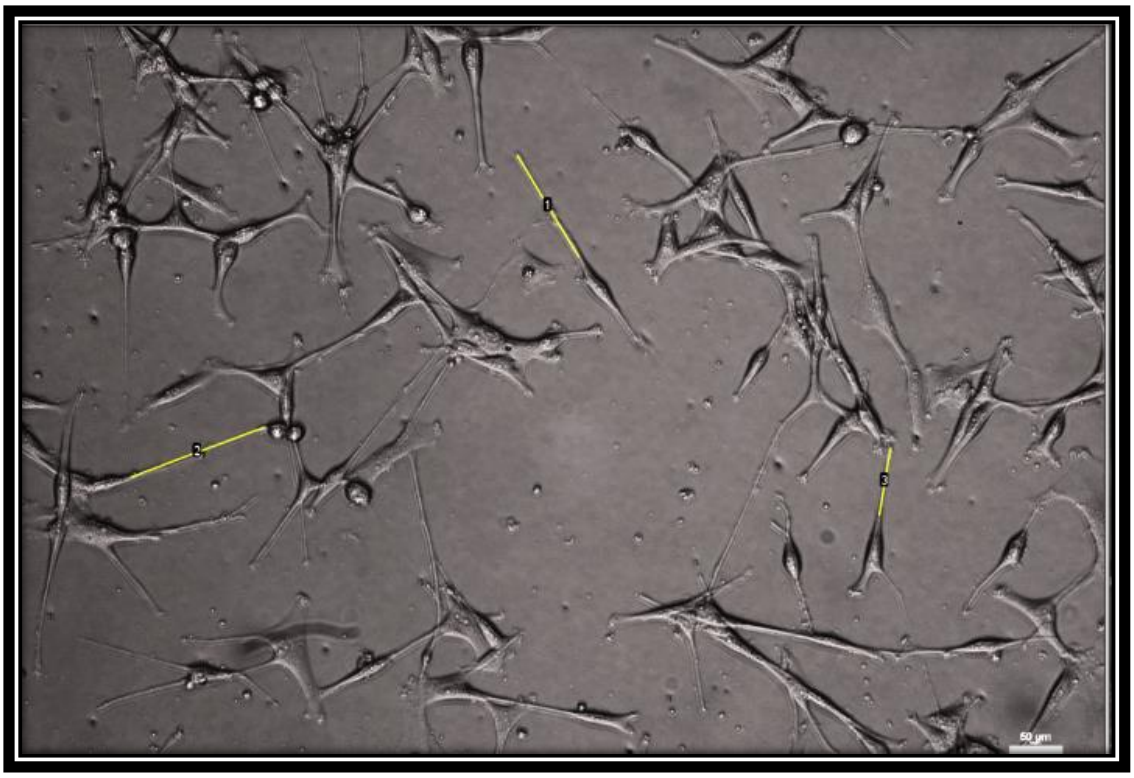

Figure 3. U87MG-wt cell line TMs at 20x magnification. TMs length was counted as shown with the yellow line.

5.1.b. 3D *in vitro* cell cultures

- ***Generation of 3D multicellular spheroids***

3D multicellular spheroids were generated using the Ultra-Low Adherence U–bottom plates (ULA- plates). For each cell type, a single-cell suspension of approximate cell density 600cells/100ul of $DMEM^{++}$ was seeded per well in a 96-well ULA plate. To mimic intratumoral heterogeneity, U87MG-PML OE and U87MG-shPML cell constructs were also co-cultured to generate 3D spheroids at an initial ratio of 1:1. The evolution and growth pattern of the spheroids were monitored over a total period of 21 days by capturing brightfield micrographs using an Eclipse Ts2R inverse wide-field optical microscope (Nikon Instruments, Tokyo, Japan). For all spheroids, images were acquired every 3 days. Image analysis was performed using the Fiji Software where the radius of the core area was estimated.

- ***Invasion assay***

In order to study the invasive physiological characteristics of the different cell lines, an invasion protocol previously described by Oraiopoulou et al., 2018 was performed. After the aggregation process was completed, the multicellular spheroids were transferred in a U-bottom plate within an ECM-like substrate. The invasion solution contained ice-cold BME Pathclear (Amsbio, Cultrex ®, UK) diluted in supplemented DMEM at final concentration 1:1. The U-bottom plate was centrifuged for 5min at 300rpm at 4^{o}C, in order to place the spheroids at the center of each well, homogeneously distribute the invasive substrate and eliminate any bubbles within it. After 1h of incubation at 37^{o}C for solidification of the invasive substrate, warm culture medium was added per well and replenished when needed. The expansion and the invasive morphology adopted by the spheroids was monitored over time using an Eclipse Ts2R inverse wide-field optical microscope (Nikon Instruments, Tokyo, Japan) and confocal microscopy. For the U87MG-PML OE cells, the PML expression was monitored using the DsRed monomer distribution. DsRed monomer was fused with the PML protein and therefore reported its presence and it was excited at 514nm. Furthermore, the U87MG-ShPML cells were treated using the PKH67 green fluorescent dye (Sigma-Aldrich, Germany) and it was excited at 488nm.

5.2. *Ex vivo* brain slices cultures

5.2.a. Brain slice acquisition and culture

Brain slices were acquired from 1- to 6-month-old C57BL/6J mice. The mice were euthanized using cervical dislocation and decapitated. Following dissection, the brains were glued to the chuck of a water-cooled vibratome and trimmed close with a commercial shave razor. Under aseptic conditions, 300-400 μm thickness whole-brain sections were acquired and carefully placed in 0.4-μm membrane inserts (Millipore PICM0RG50) in a 6-well plate. The transfer of the slices was facilitated by a brush. Brain slices (1– 3 per well depending on size) are cultured in 6-well plates at 37°C and 5% CO_2 and are incubated for minimum two weeks while others were used for acute transplantation of spheroids. 1ml of brain slice medium per well was added. The medium was refreshed after 3-4 h and then every 24h. The brain slice medium is composed of DMEM containing: F12+L-glutamine (2,5mM), HEPES (15mM) + Sodium bicarbonate (14mM), 25% heat-inactivated horse serum, Gentamicin 1‰. To prevent dehydration the tissue was moistened with a drop of medium every day, and remaining excess medium removed.

5.2.b. Spheroid implantation

GBM spheroids were generated using the method described in section 4.3.a. GBM spheroids were implanted into the brain slices upon formation. Two spheroids per brain slice were manually implanted using a 200µlt pipette under a stereoscope. Spheroids were implanted in both hemispheres and incubated at 37°C under the standard conditions. Following implantation, medium was refreshed and the slices cultivated at 37 °C and 5% CO_2 until further use. The whole procedure is depicted in *Figure 4*.

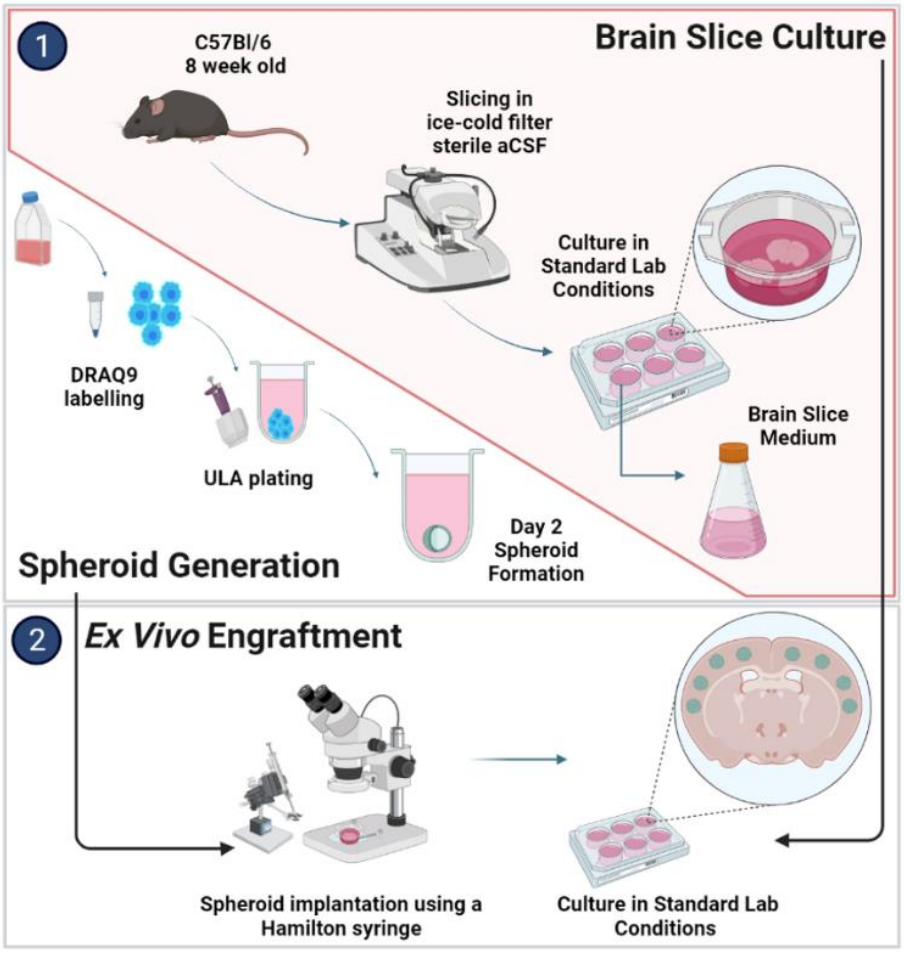

Figure 4. Ex vivo brain slice culture and spheroid implantation procedure.

5.2.c. Brain slice imaging and invasion

The *ex vivo* invasion was allowed to proceed for 72h, after which the implanted brain slices were fixed and imaged using confocal microscopy. For fixation, brain slice medium was removed from the wells and 1,5 ml 4% paraformaldehyde (PFA) was added on top of the filter for 1,5 h at RT. Fixed slices were transferred onto a microscope- slide. On top of the slice, mounting medium, containing DAPI (4',6-

diamidino-2-phenylindole; ibidi, USA) as a counterstain to label cell nuclei, was added (5 to 6 drops- enough to cover the whole slices). Slices were covered with a coverslip and secured with nail polish. Brain slices were imaged using a confocal laser scanning microscope (SP8 X, Leica, Germany) in 10x and 40x magnification scanned at 405 nm (DAPI). All images are Z-stack and maximum intensity projection with a step size ranging between 1 to 5µm. Migratory cells were visible as spikes emerging from the bulk of the spheroids that had been formed by cells establishing an infiltration path.

6. RESULTS

In this study, we assessed the cell growth and invasion over time of U87MG cell lines U87-PML OE, U87MG-ShPML) modified with respect to PML expression. The U87MG-wt and U87MG- PML cell lines were used as control. The growth properties were studied in both 2D and 3D conditions, while the invasive properties were studied exclusively in 3D, where cell migration was fully ECM-dependent. We further investigate the effect of TM-network on proliferation for all the cell lines in 2D cultures. To further unravel the role of TM- network in GBM proliferation and treatment, GJ channel blocker, CBX was tested both alone and in combination with chemotherapeutic drug TMZ in 2D cell cultures.

6.1. Cell proliferation and Spheroid growth

6.1.a. Proliferation /Doubling time estimation

In principle, glioma cells proliferate with doubling time ranging from 24h to a couple of days (Oraiopoulou et al., 2017). Specifically, for the U87MG-wt cells, their population doubling time is estimated at ~30h as provider's recommendations ATCC® HTB-14™, USA and further reports (Oraiopoulou et al., 2017). Furthermore, the spontaneous cell death of the U87MG-wt has been reported at 6% (Hambsch et al., 2017). In this work the doubling time and cell viability of all the cell lines was estimated.

The doubling time and cell viability of all cell lines was estimated in 2D cell cultures using the trypan blue exclusion viability assay. The measurements are presented in *Table 1*. The average doubling time of the U87MG-wt and the U87MG-PML cell line was estimated at approximately 41h and 54h and the intrinsic cell death at 15% and 20% respectively.

The proliferation time of the U87MG-PML OE cell line was estimated at approximately 85h and the intrinsic cell death at 20% while the doubling time for U87MG-shPML cells was estimated at 55h. In line with previous studies [ref], the U87MG-PML OE cells exhibited slower growth dynamics. The presence of the antibiotic did not considerably affect the growth rate or the spontaneous cell death rate in either of the cell types.

Remarkably, continuous treatment with antibiotic doxycycline led to the emergence of a PML-resistant cell line, which exhibited a doubling time of 63h. *Figure 5* displays the cell counts of all the studied cell lines across all the experiments (depicted with blue dots). The best fit curves are depicted with red line in Figure 5. The least-squares fitting methods is used to estimate the coefficients of the regression model (one-term exponential) and estimate the respective doubling times.

Cell Line	Average Doubling Time (in hours)	Spontaneous cell death (%)
U87MG-wt	**41**	**15**
U87MG-PML	**54**	**20**
U87MG-PML OE (PML –non resistant)	**85**	**20**
U87MG-PML OE (PML - resistant)	63	20
U87MG-shPML	**56**	**25**

Table 1. Doubling time and spontaneous cell death mean estimates for the GB studied cell lines.

The best fit curves from all doubling time experiments for each cell line are presented below. Blue dots represent the cell population over time for each experiment. Red lines represent the best fit curve.

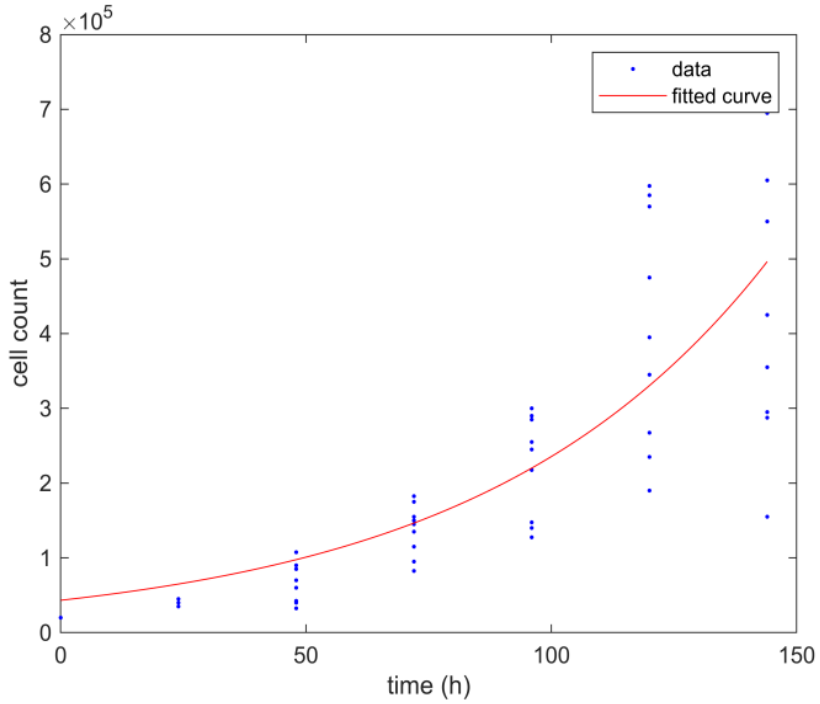

U87MG-wt doubling time data

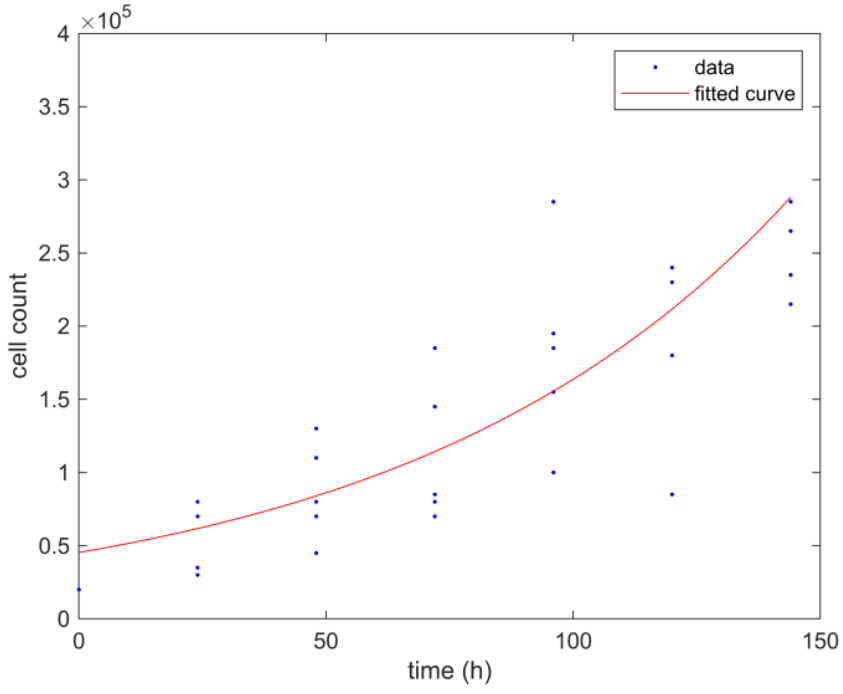

U87MG-PML doubling time data

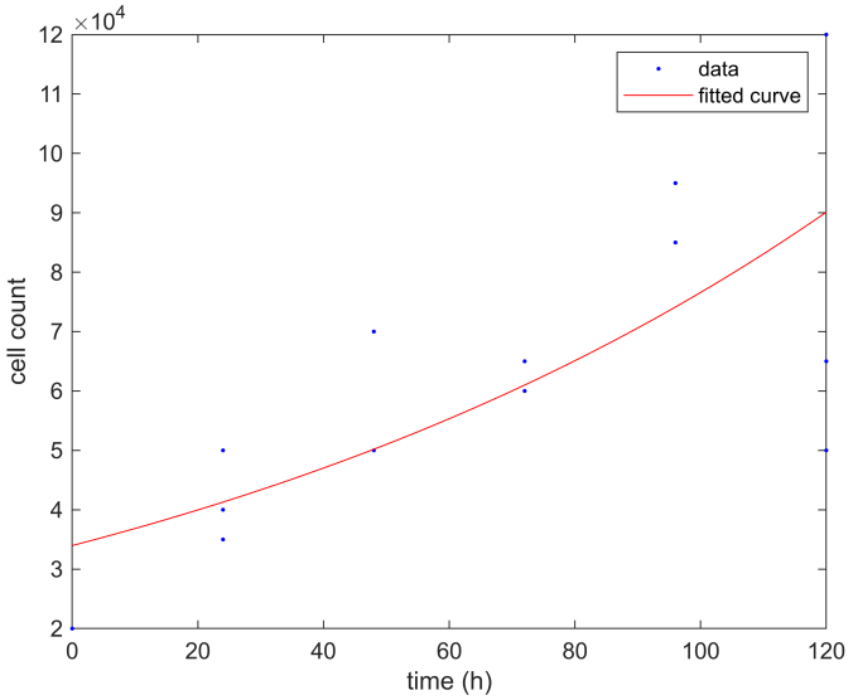

U87MG-PML OE doubling time data

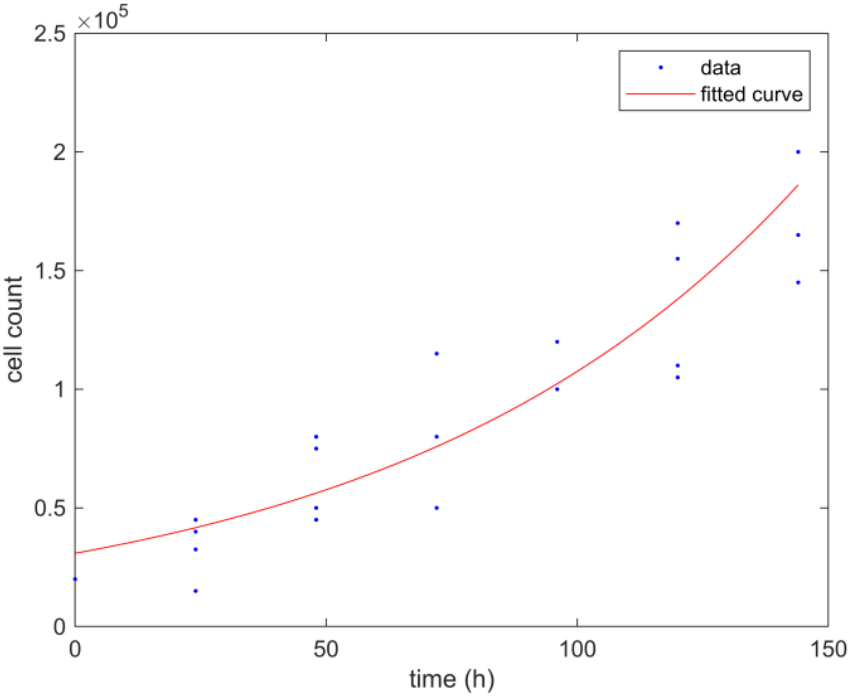

U87MG-Sh PML doubling time data

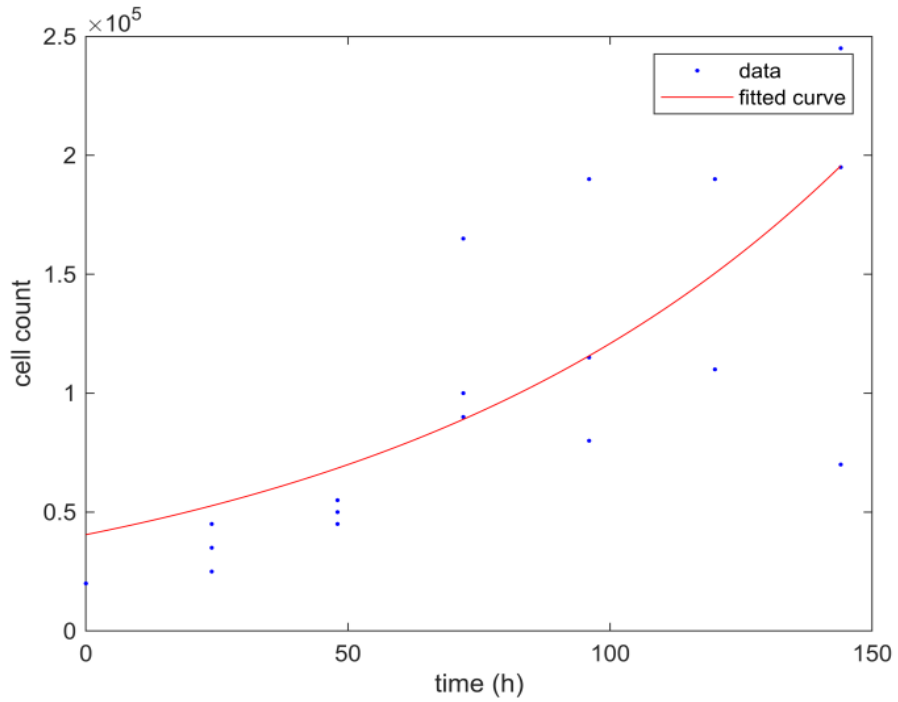

U87MG- PML resistant data

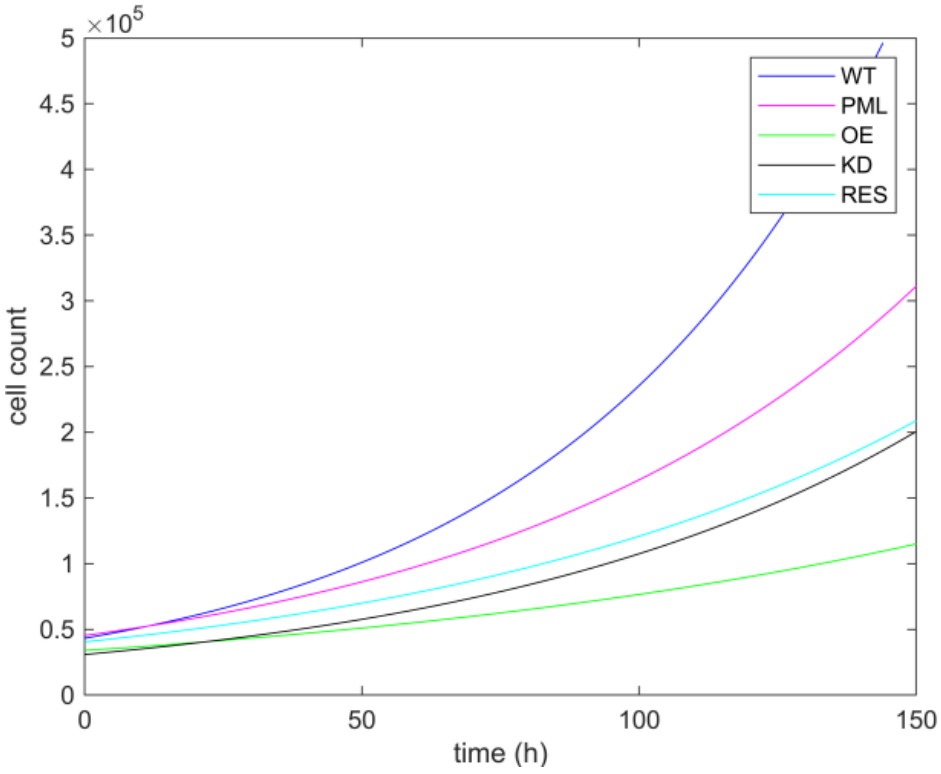

Figure 5. Growth evolution curves representing the best fit for each cell line overtime.

6.1.b. Spheroid growth expansion

3D multicellular spheroids were generated using ULA surface coating plates that minimizes cell adherence to allow spheroid formation. Optical microscopy was used to monitor the growth of the spheroids over time. Brightfield micrographs were captured in predefined time intervals, in order to estimate the area expansion of the tumor.

All cell lines approximately needed 48 hours from plating to spheroid formation (zero day). U87MG-PML OE cells exhibited slower aggregation capacity, with deformed tumor boundaries and less compactness as depicted in bright field images (*Fig.6*). Growth curves represent the radial expansion over time (*Fig.7*). It can be observed that the U87MG-PML OE cells exhibited significantly slower growth dynamics, as also indicated in the 2D experiments.

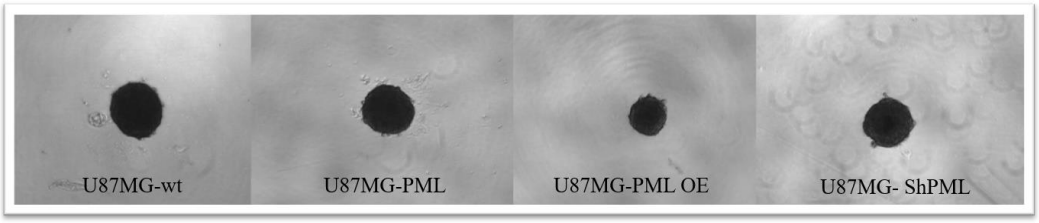

Figure 6. Representative bright field images of the spheroid morphologies in the ULA plate on day 7 at 4x magnification, scale bar is set at 100 μm.

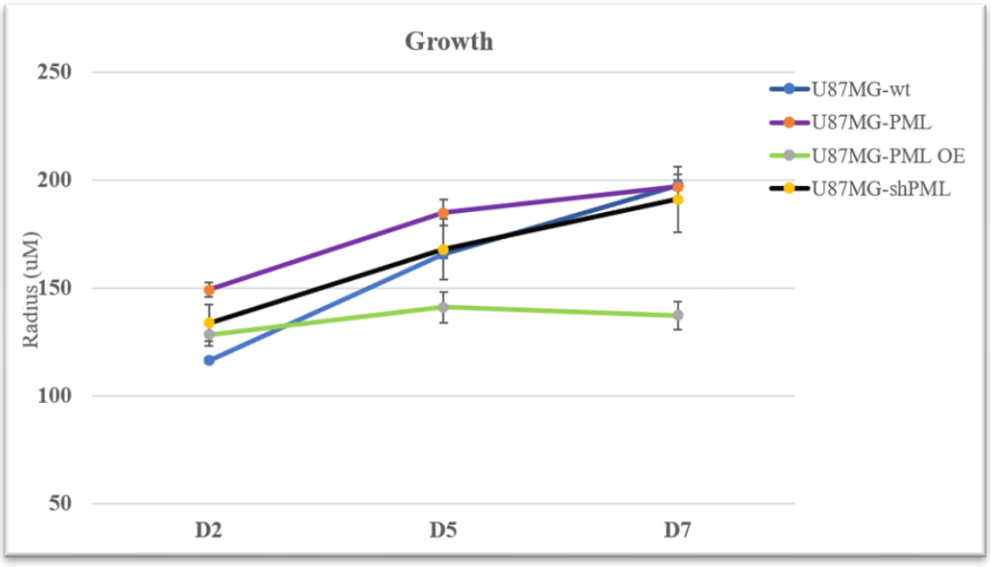

Figure.7. In vitro spatiotemporal growth curves representing the radial expansion of the spheroids in the ULA plate overtime.

6.2. Spheroid invasion

6.2.a. Invasion in an ECM-matrix

To investigate the invasive properties of the spheroids, the invasion process was conditionally allowed by transferring the respective spheroids in an ECM-like substrate environment. Optical microscopy was employed every 24h to monitor the invasive pattern of the spheroids of each cell type for up to 10 days. The invasive capacity of the spheroids was qualitatively assessed in this work through morphological characterization, focusing on the adopted pattern and the radial expansion of the invasive rim.

In *Figure 8* the invasive morphology of the cell lines U87MG-PML OE and U87MG-shPML is depicted. The invasive morphology of a co- culture spheroid of U87MG-shPML and U87MG-PML OE is depicted as well. The U87MG-PML OE cells exhibited the typical starburst invasive morphology (Oraiopoulou et al., 2018) and demonstrated a highly invasive capacity, even though the core of the invasive spheroid was significantly smaller compared to the control cell lines. In contrast, the U87MG-shPML exhibited limited invasive capacity. Interestingly, in the co-culture condition, both cell lines exhibited invasive capacity, suggesting that the invasive cell line facilitates the invasion of the non-invasive cell line or more specifically, indicating a potential interaction between them.

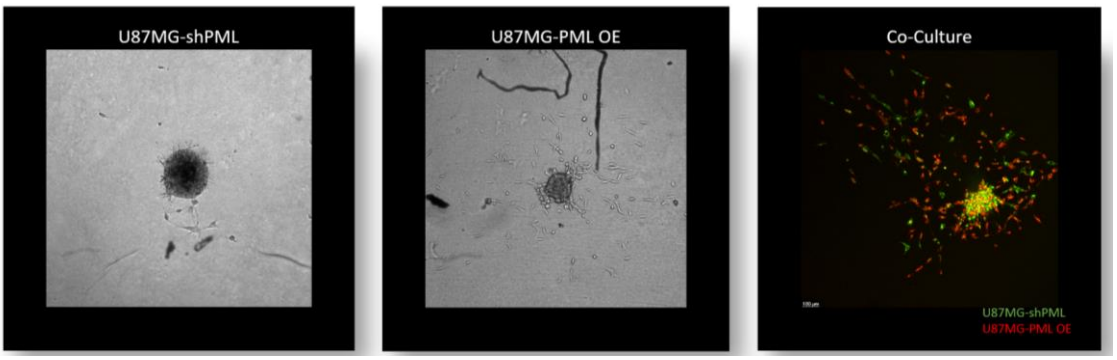

Figure 8. Bright field and confocal z-stack maximum projection images of representative spheroids at 24h of in vitro invasion at 10x magnification. U87MG-ShPML cells are shown with green while U87MG-PML OE cells are shown with red.

6.2.b. Invasion in *ex vivo* conditions

To better mimic the tumor microenvironment of GBM, organotypic brain slices from mice were utilized as the invasion matrix for implanted spheroids. Spheroid's invasion was imaged by confocal microscopy. Interestingly, all cell lines exhibited invasive capacity when cultured on brain slices, as depicted in Figure 9. The invasive pattern of spheroids displayed the characteristic starburst morphology observed in *in vitro* cultures. Particularly noteworthy is the observation that U87MG-PML OE spheroids displayed extensive invasion, with the core deformed and spreading throughout the brain slice.

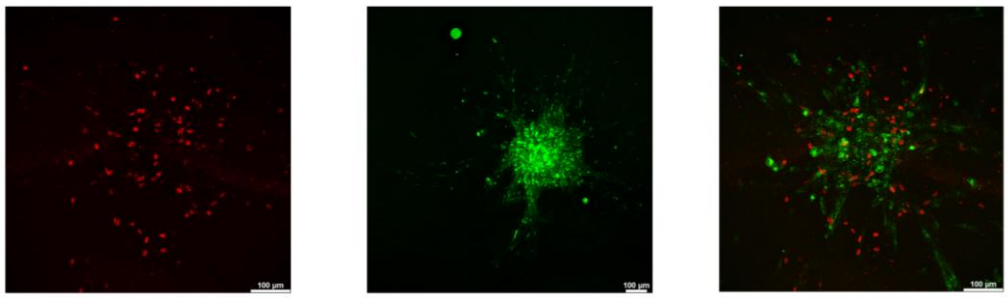

Figure 9. Representative confocal images of implanted spheroids. U87MG-PML OE invasion (left), U87MG-ShPML invasion (center), Co-culture spheroid of U87MG-PML OE and U87MG-ShPML invasion. Scale bar is set at 100 μm.

6.3. Tumor Microtubes (TMs) network

To further investigate the role of the PML protein in the TM-network of GBM, 2D cultures of all cell lines were used. *Figure 10* displays representative brightfield images of all cell lines at indicative days 3 and 5.

In *Figure 11*, the average total number of TMs for all cell lines is presented up to day 3. Notably, the U87MG -PML OE cell line exhibits a smaller number of TMs compared to others. To further elucidate these differences, a multi-comparison statistical test was conducted among the different groups (*Figure 11b)*. The results, including the corresponding p-values for hypothesis testing whether the mean difference is zero, are summarized in Table 2. Specifically, significant differences were found between U87MG-wt and the other cell lines, as well as between U87MG-PML OE and U87MG-shPML.

In *Figure 12*, the average length of connected and unconnected TMs is illustrated. To assess differences across the entire set of samples among different cell lines, a non-

parametric Kruskal-Wallis statistical test was employed. The results of this analysis, including the corresponding p-values, are summarized in a table provided. However, no statistically significant difference in the mean length of TMs between connected or unconnected TMs was observed.

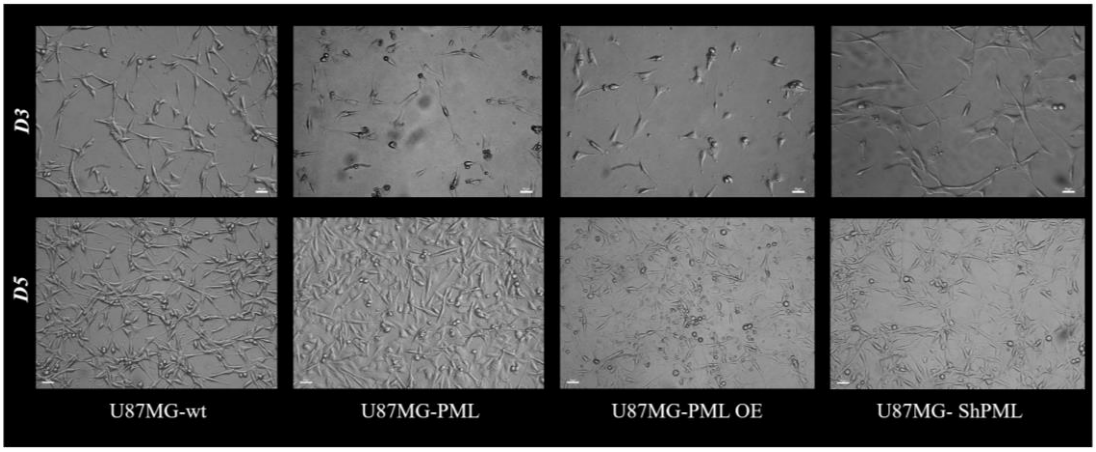

Figure 10. Representative bright- field images of TMs network for each cell line on day 3 and day 5 at 20x magnification.

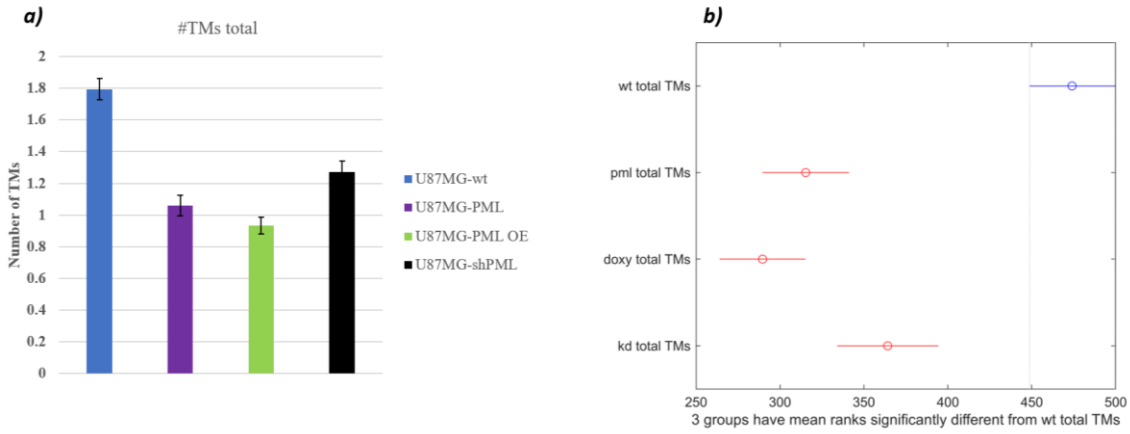

Figure 11. *a)* The average total number of TMs up to day 3 is presented for all cell lines, b) Kruskal Wallis test.

Group A	Group B	Lower Limit	A-B	Upper Limit	P-value
1	**2**	**107.5872**	**158.6516**	**209.7160**	**0**
1	**3**	**133.4685**	**184.3300**	**235.1915**	**0**
1	**4**	**54.3665**	**109.7742**	**165.1818**	**0**
2	3	-25.7089	25.6784	77.0657	0.5733
2	4	-104.7681	-48.8774	7.0133	0.1109
3	**4**	**-130.2612**	**-74.5558**	**-18.8504**	**0.0033**

Table 2. Multiple comparison results of total number of TMs among the different cell lines. The first two columns show the groups that are compared (1: WT; 2: PML; 3: PML-OE; 4: PML-KD). The fourth column shows the difference between the estimated group means. The third and fifth columns show the lower and upper limits for 95% confidence intervals for the true mean difference. The sixth column contains the p-value for a hypothesis test that the corresponding mean difference is equal to zero. Therefore, these results suggest that the data in group 1 comes from a different distribution, and the data in groups 3 and 4 also come from a different distribution.

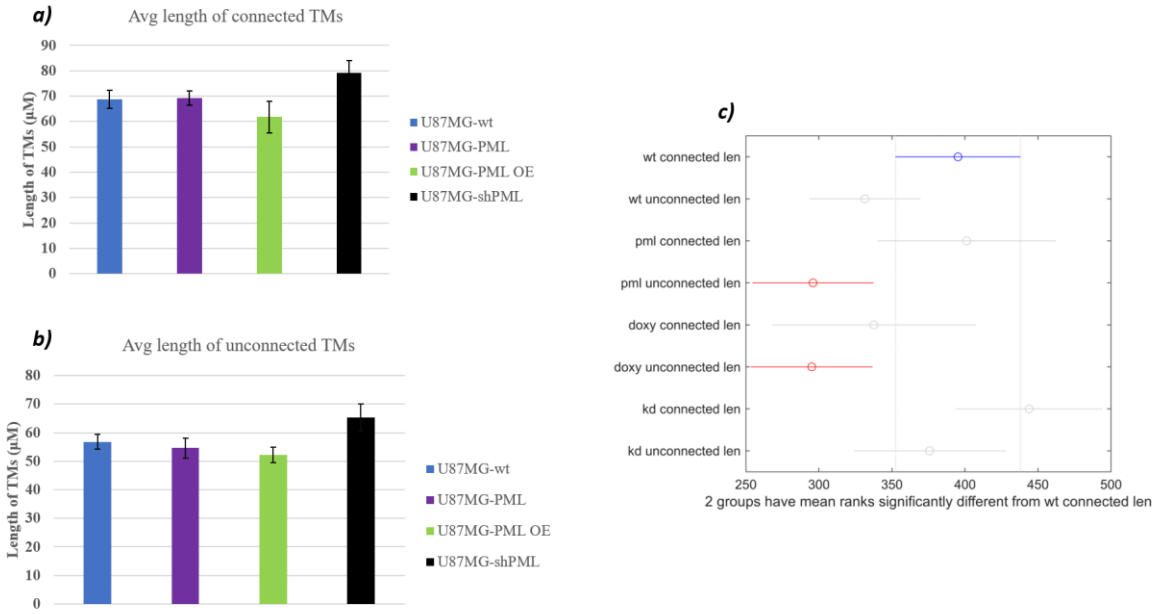

Figure 12. For all the cell lines the average length of a) Connected TMs, b) unconnected TMs is depicted, c) Kruskal Wallis statistical test over all connected and unconnected TMs cell lines

Group A	Group B	Lower Limit	A-B	Upper Limit	P-value
1	2	-16.0499	63.7634	143.5768	0.2308
1	3	-110.3682	-5.9760	98.4162	1
1	4	15.5432	99.2431	182.9431	0.0079
1	5	-55.7742	57.5700	170.9143	0.7860
1	6	16.0735	100.1391	184.2046	0.0074
1	7	-141.7751	-48.6637	44.4478	0.7601
1	8	-75.6076	19.4163	114.4403	0.9986
2	3	-169.7531	-69.7394	30.2743	0.4060
2	4	-42.6913	35.4797	113.6507	0.8686
2	5	-115.5184	-6.1934	103.1315	1
2	6	-42.1866	36.3756	114.9379	0.8561
2	7	-200.6017	-112.4271	-24.2525	0.0028
2	8	-134.5389	-44.3471	45.8447	0.8130
3	4	2.0771	105.2191	208.3610	0.0417
3	5	-64.8265	63.5460	191.9185	0.8076
3	6	2.6762	106.1150	209.5539	0.0396
3	7	-153.6035	-42.6877	68.2282	0.9414
3	8	-87.1338	25.3923	137.9184	0.9974
4	5	-153.8669	-41.6731	70.5207	0.9514
4	6	-81.6119	0.8959	83.4038	1
4	7	-239.6144	-147.9068	-56.1992	0
4	8	-173.4755	-79.8268	13.8219	0.1618
5	6	-69.8977	42.5691	155.0359	0.9463
5	7	-225.6134	-106.2337	13.1460	0.1233
5	8	-159.0309	-38.1537	82.7236	0.9802
6	7	-240.8441	-148.8027	-56.7614	0
6	8	-174.6983	-80.7227	13.2528	0.1545
7	8	-34.0677	68.0800	170.2277	0.4681

Table 2i. Multiple comparison results of connected and unconnected TM lengths among the different groups. The first two columns show the groups that are compared (1: WT-connected; 2: WT-unconnected; 3: PML-connected; 4: PML-unconnected; 5: PML-OE-connected; 6: PML-OE-unconnected; 7: PML-KD-connected; 8: PML-KD-unconnected).

6.4. Effect of TM-network on GBM proliferation

In order to study the effect of the TM-network on GBM proliferation, the U87MG-wt cell line was treated with the GJ channel blocker, CBX. Various concentrations of CBX were used, as shown in *Figure 13*. Concentrations of 50 μM and 75 μM did not affect the proliferation time. The optimum concentration was found to be around 100 μM, where the doubling time is doubled in comparison with the control cell lines, while the

spontaneous cell death rate remained almost unaffected. *Figure 13b* shows the temporal evolution of the cell population for different concentrations of the CBX. The growth curve of the100 μM concentration of CBX, depicted with the yellow line, exhibited slower growth dynamics. Concentrations of CBX above 100 μM had a drastic effect on the cell population.

a)

U87MG-WT Concentrations of CBX (uM)	Average Doubling Time (in hours)	Spontaneous cell death (%)
Control	30	4,8%
50	31	5,5%
75	30	2,8%
100	66	5,8%
130	485	*
160	*	*

*N/A

b)

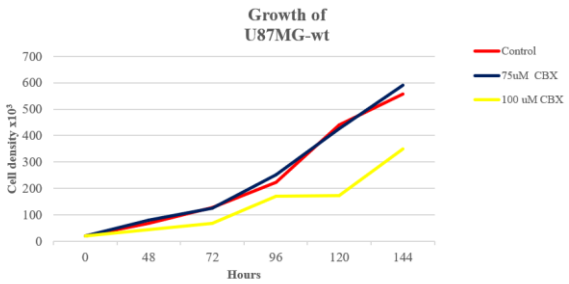

Figure 13. *a)* **Table 3**. Different concentrations of CBX for U87MG-wt cell line, their average doubling time and the spontaneous cell death. b) Growth curves of U87MG - wt for 75 μM and 100 μM of CBX over time.

6.5. GBM network resistance: Combination treatment of CBX and TMZ

To investigate the effect of TM- network on GBM treatment, a combination of the gap junction inhibitor CBX and TMZ, the standard chemotherapeutic treatment for GBM, was utilized. TMZ was administered at a concentration of 500 μM, which is the IC50 for U87MG-wt. Two different concentrations of CBX were tested, 75 μM and 100 μM. Cell proliferation was monitored over time in the U87MG-wt cell line.

Unfortunately, the concentration of TMZ was too high for continuous treatment, hindering the observation of any synergistic effect with CBX. As shown in *Figure 14*, the cell population growth was significantly inhibited by treatment with TMZ or the gap junction inhibitor combined with TMZ.

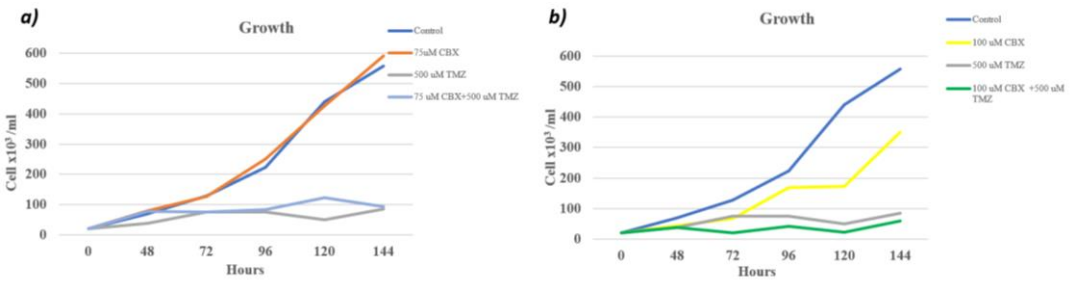

Figure 14. Growth curves of U87MG -wt cell line for combination treatment of: a) 75uM CBX and 500uM TMZ and their controls, b) 100uM CBX and 500uM TMZ and their controls.

7. DISCUSSION

In this work, the role of the PML protein in GBM growth, invasion and TM communication network is investigated. To achieve this, the well-established U87MG-wt cell line is modified to overexpress or silence the PML protein. Both 2D and 3D biological models have been utilized. The invasive capacity of the PML-modified cells lines was tested both *in vitro* and *ex vivo* in murine brain slices. The effect of the TM - network on GBM proliferation and treatment response is also explored. Optical and confocal microscopy are used to monitor the phenomena.

PML OE inhibits growth and promotes GBM cell invasion. The U87MG-PML OE cells in 2D cultures exhibited increased proliferation time compared to the control cell lines in the doubling time/trypan blue viability assay experiments. The proliferation time of the cell population can be influenced by various factors affecting their growth properties. The spontaneous/intrinsic cell death rate, for example is a key characteristic of each cell line and contributes to the progression of the tumor. The PML IV isoform acts as a regulator of apoptosis, cell-cycle arrest, senescence and DNA damage by the p53 protein activation (Nisole et al., 2013). However, the trypan blue viability assay, revealed no significant differences in the spontaneous cell death rates between the U87MG-PML OE cells and the controls, suggesting that the prolonged proliferation time is not attributed to an increased cell death pattern. Instead, it indicates a potential cell-cycle arrest. Our results align with previous findings, indicating that PML OE results in decreased proliferation rate and cell-cycle restriction (Iwanami et al., 2013; Sachini et al., 2019).These studies propose the cell-cycle arrest in the G0/G1 fraction; however, they refer to different PML isoforms or biological cancer models.

Additionally, in the case of 3D models, U87MG-PML OE cell line generated smaller spheroids. All these findings are is in line with previous reports, indicating that PML IV reduces cell aggregation and sphere formation due to its inhibitory effect on the cancer stem cells and their self-renewal capacity (Sachini et al., 2019). Moreover, U87MG-PML OE cells exhibited significantly slower growth dynamics, as also indicated in the 2D experiments.

Furthermore, U87MG-PML OE exhibited highly invasive capacity even though the core of the U87MG-PML OE spheroidas smaller and deformed over time. The invasive pattern adopted the typical starburst morphology (Oraiopoulou et al., 2018). The tumor core exhibited a slight reduction in size during the first invasive time points. This slight reduction is possibly attributed to a higher migratory and a lower proliferative capacity of the U87MG-PML OE cells. The same pattern was observed in implanted spheroids in the organotypic brain slices where the U87MG-PML OE exhibit invasive capacity as well. These findings indicate that upon PML presence, tumor growth and migration appear to have antagonistic roles. PML exhibits a pro-migratory behavior and PML OE cells seem to prefer migration rather than proliferation. Our results are in line with previous findings that set PML as a regulator of both growth, inducing growth inhibition (Iwanami et al., 2013; Amodeo et al., 2017), and migration (Amodeo et al.,

2017). We observed that the organotypic brain slices facilitate further the invasive capacity of GBM cells. Overall, the maintenance of invasive patterns in both *in vitro* and *ex vivo* affirms the consistency of our observations in the more physiologic realistic environment.

PML OE and KD co-culture: dynamic interplay. Interestingly, *in vitro,* we observed that the invasive capacity of U87MG-ShPML changes when co-cultured with U87MG-PML OE. The U87MG-PML OE cell line exhibited highly invasive capacity in the ECM-like matrix, while U87MG-ShPML showed limited invasion. In the case of co-culture, both cell lines exhibited invasive capacity, indicating further interactions between the two sub-clones. We hypothesize that the U87MG-PML OE cells secrete factors that induce the invasion in U87MG-Sh PML cells through chemotaxis or haptotaxis, shaping the ECM and creating paths for migration. Another possible reason is a phenotype switching between the cell lines. Additionally, the fact that the two sub-clones interact and one changes behavior introduces extra controls that need to be performed during patient classification (e.g., spatial transcriptomics during biopsy, in vitro spatiotemporal checks, etc.). Further investigation is crucial to understand any potential interactions between these cell subpopulations and their contribution to the invasion mechanism. Identifying the underlying mechanisms is essential for a comprehensive understanding of the impact of heterogeneity on invasion. Additionally, targeting the reciprocal communication and cooperation underlying these interactions may present new therapeutic opportunities.

PML may affect GBM network. The ability to interconnect via ultra-long and highly functional TMs is an important mechanism of progression and resistance in gliomas. The resulting multicellular network is able to communicate via Cx43 gap junction connections (Osswald et al., 2015). We would like to investigate whether PML affects glioma network. In this work, we explored structural differences in TM network connectivity among the different cell lines. The U87MG-wt generated a higher number of TMs in comparison with all the other cell lines indicating that the PML -modified cell lines affect the GBM network. U87MG -PML OE cell line formed a smaller number of TMs in comparison with the U87MG-shPML indicating that PML affects the network formation through TMs. However, no correlation has been found between the average length of connected and unconnected TMs of cell lines.

TM network affects GBM growth. This study aims to identify the extent to which the TM network affects the growth rate of GBM cells and whether it contributes to therapy resistance in our cell lines. As a proof of concept, we tested the effect of GJ inhibitor, CBX, in different concentrations on the growth of U87MG- wt cell line. We observed that the inhibitory effect was greater at a concentration above 100 μM, while smaller concentrations didn't seem to affect proliferation. Specifically, CBX increased cell doubling time from 30 hours to 66 hours. These findings indicate a strong correlation between gap junction inhibitory activity and anti-tumor effect, or equivalently between

the TM network and cell population growth. Various i*n vitro* and *in vivo* studies have shown that CBX treatment increased tumor latency and median survival compared to the control treatments (Hitomi et al., 2015; Mettang et al., 2018). Treatment with CBX to the standard treatment for GBM has the potential to improve the therapeutic window, both temporally and spatially. Gap junction inhibitors augmented the anti-tumor effect of TMZ in both subcutaneous and orthotopic xenograft models (Hitomi et al., 2015).

8. FUTURE PERSPECTIVES

GBM exhibits diverse molecular and cellular profiles, both within and among individuals, demonstrating significant heterogeneity. It is characterized by excessive proliferation and infiltration that destroy normal brain regions and impair brain function. GBM's intrinsic heterogeneity, along with bidirectional communication between glioma cells and the brain tumor microenvironment, promotes growth and invasion, while also conferring resistance to treatment. Much remains to be unraveled regarding the fundamental biology behind neuron-glioma interactions and how genetic, epigenetic, and microenvironmental cues that drive heterogeneity affect GBM progression and response to treatment.

In this work, we focus on the PML protein. PML is an important regulator of apoptosis, cell cycle, and DNA damage responses. PML also functions in neuronal development and brain cognition processes. Furthermore, independently of its ability to control proliferation, PML also controls cell migration in both normal settings and GBM pathology.

One of the key obstacles in research advancements for GBM treatment is the challenge of faithfully replicating the intricate brain microenvironment through preclinical models. In this work, we explore the role of PML in GBM growth, invasion, glioma network formation, and treatment, utilizing a variety of models including 2D/3D *in vitro* cultures and *ex vivo* models, and monitoring the phenomena through wide-field and confocal microscopy. Our work demonstrates the role of PML in growth, invasion, clonal interplay, and TM connectivity and establishes the experimental setups for further investigations.

In the future, we will utilize the *ex vivo* setup to focus on the spatiotemporal evolution of the GBM spheroids, quantifying and further unraveling the intricate dynamics of their progression and heterogeneity. We seek to elucidate how the tumor cell populations spatially distribute within the brain slice and how the anatomical structure of the brain can affect the evolution of the tumor. Additionally, we will focus on investigating the effects of neuronal activity perturbation on spheroid progression through various treatment interventions in the brain slices.

Additional experiments and advanced segmentation methods are important to validate our primary observations regarding the connectivity differences observed in our cell lines. Apart from the structural differences of the TM network investigated here for the various cell lines, it is important to explore also the functional communication of the GBM cells and characterize their Ca2+ communication patterns. Ca2+ pulses serve as "calcium codes" differing in magnitude, time and frequency. Ca2+ pulses affect cell division process, genomic instability and invasion. GBM cells also project tumor microtubes contact with neurons, and exchange signaling molecules to promote their expansion. Thus, targeting signaling and synaptic components of GBM progression has been proposed as a therapeutic strategy against glioblastoma. We aim to test the response of our GBM cell lines to various concentrations of TMZ in combination with the gap junction inhibitor. In our future research pursuits, we are poised to delve into

the tumor connectivity, with a particular focus on elucidating the structural and functional attributes of GBM and neuroglioma networks. Our investigations aim to unravel the underlying mechanisms governing the formation and dynamics of these networks, shedding light on their role in tumor progression and therapeutic response.

In addition, we aim to explore the mechanisms that facilitate the invasion of the PML KD clone when co-cultured with the PML OE cells. Secretion factors and phenotype switching mechanisms will be explored as potential explanations for the observed cooperative invasion. We also seek to understand how these factors might be affected when spheroids grow on organotypic brain slices.

Finally, we aim to employ mathematical/computational models in the future to integrate and quantify the complex phenomena we observe. The ultimate goal is to illuminate the intricate mechanistic aspects of GBM that are challenging to isolate experimentally, offering invaluable guidance for experimental design and providing rigorous predictions of GBM progression and optimal treatment solutions. This can only be truly achieved provided these *in silico* methods can be calibrated and validated with *in vitro*, *ex vivo*, and *in vivo* experimental data. Through the integration of computational models with experimental data, we aim to elucidate the complex interplay between growth, invasion, connectivity, and pharmacodynamics in tumors. By manipulating key parameters such as doubling time, number of connections, and drug inhibition, we seek to unravel the fundamental principles governing tumor behavior and therapeutic response, facilitating the design of more targeted and personalized treatment strategies.

9. THESIS LIST OF PUBLICATIONS

Posters

- Maria Tampakaki, Eleftheria Tzamali, Giorgos Tzedakis, **Eirini Makrygiannaki**, Mikis Mylonakis, Evangelos Marakis, Giannis Zacharakis, Vangelis Sakkalis, Joseph Papamatheakis "***Brain cancer evolution under the prism of intra-tumoral heterogeneity***", 18th European Molecular Imaging Meeting, 14-17 March,2023, Salzburg, Austria
- **Eirini Makrygiannaki,** Maria Tampakaki, Eleftheria Tzamali, Giannis Zacharakis, K.Sidiropoulou, Vangelis Sakkalis, Joseph Papamatheakis "***Modeling PML-mediated Glioblastoma Growth Dynamics: Insights from Spheroid Based Studies and Brain Tissue Slice Implantation***", 2nd International Conference on Nanotechnologies & Bio nanoscience (NanoBio 2023), September 11-15 2023 Heraklion Crete Greece
- Maria Tampakaki, Eleftheria Tzamali, **Eirini Makrygiannaki**, Giorgos Tzedakis, Mikis Mylonakis, Evangelos Marakis, Kyriaki Sidiropoulou, Vangelis Sakkalis, Joseph Papamatheakis, Giannis Zacharakis "***A Tripartite Approach through In Vitro, Ex Vivo, and In Silico Modeling for Deeper Understanding of Glioblastoma***",19th European Molecular Imaging Meeting (EMIM), 2024, Porto, Portugal

10. ACKNOWLEDGEMENTS

Η παρούσα εργασία με θέμα «**PML-mediated Glioblastoma Growth Dynamics: Insights from Spheroid-Based Studies and Brain Tissue Slice Implantation** » πραγματοποιήθηκε στο πλαίσιο της μεταπτυχιακής εργασίας του διιδρυματικού προγράμματος « Biomedical Engineering» το έτος 2022-2024.

Αισθάνομαι την ανάγκη να εκφράσω τις ειλικρινείς και θερμές ευχαριστίες μου σε όσους συνέβαλαν στην ολοκλήρωση αυτής της προσπάθειας. Πρώτα από όλα, θα ήθελα να ευχαριστήσω τον επιβλέποντα μου Ερευνητή Δρ. κ. **Βαγγέλη Σακκαλή** για την εμπιστοσύνη που μου έδειξε, για τη συνεχή προσφορά και καθοδήγησή του , καθώς και για τις πολύτιμες συμβουλές που μου έδωσε καθ' όλη τη διάρκεια αυτής της εργασίας. Θα ήθελα, ακόμη, να ευχαριστήσω τον Καθηγητή κ. **Σήφη Παπαματθαιάκη** για τις σημαντικές συμβουλές του, ο οποίος αποτέλεσε εμπνευστή της ιδέας και συνεχίζει να αποτελεί πηγή γνώσεων και δημιουργικότητας. Ευχαριστώ, επίσης, τον Δρ. κ. **Γιάννη Ζαχαράκη**, για όλες τις ευκαιρίες που μου έδωσε να διευρύνω τους ορίζοντές μου.

Ευχαριστώ ιδιαίτερα την κα ***Ταμπακάκη Μαρία ,*** υποψήφια διδάκτωρ, για την πολύτιμη βοήθεια της, την αμέριστη υποστήριξη, για την εμπιστοσύνη που έδειξε στο πρόσωπο μου και τον χρόνο που μου αφιέρωσε. Ακόμη, ένα μεγάλο ευχαριστώ στην Δρ. ***Ελευθερία Τζαμαλή***, η οποία με συμβούλευε και με στήριξε σε όλα τα στάδια αυτής της δουλειάς. Θα ήθελα ακόμη να ευχαριστήσω τον **Γιώργο Τζεδάκη** για την σημαντική του βοήθεια σε κομβικά σημεία αυτής της δουλειάς.

Θα ήθελα ακόμη να ευχαριστήσω την Επίκουρη Καθηγήτρια Δρ. κα **Κυριακή Σιδηροπούλου** και την ερευνητική της ομάδα, **Χρύσα Ιορδανίδου**, **Αγγελική Βέλλη** , **Λήδα Βαγιάκη**, **Κωνσταντίνο Δίσκο** και **Δρακάκη Ζωή** των οποίων η συμβολή ήταν καταλυτική για την διεκπεραίωση της εργασίας.

Τέλος, θα ήθελα να ευχαριστήσω την οικογένεια και τους φίλους μου για την υπομονή και την εμψύχωση που μου παρέχουν όλα αυτά τα χρόνια.

11. REFERENCES

Aaberg-Jessen, C. a. (2011). Invasion of primary glioma-and cell line-derived spheroids implanted into corticostriatal slice cultures. *Cancer Research*, 4305--4305.

Adamski, V. a.-F. (2017). Isolation and characterization of fast-migrating human glioma cells in the progression of malignant gliomas. *Oncology Research Featuring Preclinical and Clinical Cancer Therapeutics*, 341--353.

Alcalay, M. a. (1991). Translocation breakpoint of acute promyelocytic leukemia lies within the retinoic acid receptor alpha locus. *Proceedings of the National Academy of Sciences*, 1977--1981.

Allen, M. a. (2016). Origin of the U87MG glioma cell line: Good news and bad news. *Science translational medicine*, 354re3--354re3.

Angara, K. a. (2017). Vascular mimicry: a novel neovascularization mechanism driving anti-angiogenic therapy (AAT) resistance in glioblastoma. *Translational oncology*, 650--660.

Ascoli, C. A. (1991). Identification of a novel nuclear domain. *The Journal of cell biology*, 785--795.

Bernardi, R. a. (2007). Structure, dynamics and functions of promyelocytic leukaemia nuclear bodies. *Nature reviews Molecular cell biology*, 1006--1016.

Borrow, J. a. (1990). Molecular analysis of acute promyelocytic leukemia breakpoint cluster region on chromosome 17. *Science*, 1577--1580.

Cheng, L. a. (2013). Glioblastoma stem cells generate vascular pericytes to support vessel function and tumor growth. *Cell*, 139--152.

Claes, A. a. (2007). Diffuse glioma growth: a guerilla war. *Acta neuropathologica*, 443--458.

de Th{\'e}, H. a. (1991). The PML-RARα fusion mRNA generated by the t (15; 17) translocation in acute promyelocytic leukemia encodes a functionally altered RAR. *Cell*, 675--684.

Dellaire, G. a.-J. (2004). PML nuclear bodies: dynamic sensors of DNA damage and cellular stress. *Bioessays*, 963--977.

Flenghi, L. a. (1995). Characterization of a new monoclonal antibody (PG-M3) directed against the aminoterminal portion of the PML gene product: immunocytochemical evidence for high expression of PML proteins on activated macrophages, endothelial cells, and epithelia.

Grotzer, M. A. (2016). Dissecting brain tumor growth and metastasis in vitro and ex vivo. *Journal of Cancer Metastasis and Treatment*, 149--162.

Gurrieri, C. a.-C. (2004). Loss of the tumor suppressor PML in human cancers of multiple histologic origins. *Journal of the National Cancer Institute*, 269--279.

Jensen, K. a. (2001). PML protein isoforms and the RBCC/TRIM motif. *Oncogene*, 7223--7233.

Kiseleva, L. a. (2018). Characterization of new human glioblastoma cell lines. *Cell and Tissue Biology*, 1--6.

Klinghammer, K. a. (2017). Choosing wisely--Preclinical test models in the era of precision medicine. *Cancer treatment reviews*, 36--45.

Korb, E. a. (2013). PML in the brain: from development to degeneration. *Frontiers in oncology*, 242.

Lallemand-Breitenbach, V. a. (2010). PML nuclear bodies. *Cold Spring Harbor perspectives in biology*, a000661.

Lallemand-Breitenbach, V. a. (2018). PML nuclear bodies: from architecture to function. *Current opinion in cell biology*, 154--161.

Le, X.-F. a.-S. (1996). Analysis of the Growth and Transformation Suppressor Domains of Promyelocytic Leukemia Gene, PML. *Journal of Biological Chemistry*, 130--135.

Lei, L. a. (2011). Glioblastoma models reveal the connection between adult glial progenitors and the proneural phenotype. *PloS one*, e20041.

Lei, L. a. (2011). Glioblastoma models reveal the connection between adult glial progenitors and the proneural phenotype. *PloS one*, e20041.

Liu, C. a. (2011). Mosaic analysis with double markers reveals tumor cell of origin in glioma. *Cell*, 209--221.

Mallawaaratchy, D. M. (2015). Membrane proteome analysis of glioblastoma cell invasion. *Journal of Neuropathology \& Experimental Neurology*, 425--441.

Matsumura, H. a. (2000). Quantitative analysis of glioma cell invasion by confocal laser scanning microscopy in a novel brain slice model. *Biochemical and biophysical research communications*, 513--520.

Mazza, M. a. (2013). Is PML a tumor suppressor? *Frontiers in oncology*, 174.

Mullins, C. S. (2013). Establishment and characterization of primary glioblastoma cell lines from fresh and frozen material: a detailed comparison. *PloS one*, e71070.

N, L. D., Arie, P., Guido, R., Andreas, V. D., Dominique, F.-B., K, C. W., . . . W, E. D. (2016). The 2016 World Health Organization classification of tumors of the central nervous system: a summary. *Acta neuropathologica*, 803--820.

Nisole, S. a.-A. (2013). Differential roles of PML isoforms. *Frontiers in oncology*, 125.

Ohgaki, H. a. (2013). The Definition of Primary and Secondary GlioblastomaDefinition of Primary and Secondary Glioblastomas. *Clinical cancer research*, 764--772.

Oraiopoulou, M.-E. a. (2017). In vitro/in silico study on the role of doubling time heterogeneity among primary glioblastoma cell lines. *BioMed research international*.

Oraiopoulou, M.-E. a. (2018). Integrating in vitro experiments with in silico approaches for Glioblastoma invasion: the role of cell-to-cell adhesion heterogeneity. *Scientific reports*, 16200.

Ostrom, Q. T., Gittleman, H., Liao, P., Rouse, C., Chen, Y., Dowling, J., . . . Barnholtz-Sloan, J. (2014). CBTRUS statistical report: primary brain and central nervous system tumors diagnosed in the United States in 2007--2011. *Neuro-oncology*, iv1--iv63.

others, C. G. (2008). Comprehensive genomic characterization defines human glioblastoma genes and core pathways. *Nature*, 1061.

Perrin, S. L. (2019). Glioblastoma heterogeneity and the tumour microenvironment: implications for preclinical research and development of new treatments. *Biochemical Society transactions*, 625--638.

Previati, M. a. (2018). Functions and dys-functions of promyelocytic leukemia protein PML. *Rendiconti Lincei. Scienze Fisiche e Naturali*, 411--420.

Ram{\~a}o, A. a.-S. (2012). Changes in the expression of proteins associated with aerobic glycolysis and cell migration are involved in tumorigenic ability of two glioma cell lines. *Proteome science*, 1--12.

Regad, T. a. (2009). The tumor suppressor Pml regulates cell fate in the developing neocortex. *Nature neuroscience*, 132--140.

Ruggero, D. a.-G. (2000). The puzzling multiple lives of PML and its role in the genesis of cancer. *Bioessays*, 827--835.

Sanai, N. a.-B. (2005). Neural stem cells and the origin of gliomas. *New England Journal of Medicine*, 811--822.

Schiffer, D. a. (2018). Glioblastoma: microenvironment and niche concept. *Cancers* , 5.

Seeler, J.-S. a. (1999). The PML nuclear bodies: actors or extras? *Current opinion in genetics \& development*, 362--367.

Singh, S. K. (2004). Identification of human brain tumour initiating cells. *nature*, 396--401.

Soeda, A. a.-i. (2015). The evidence of glioblastoma heterogeneity. *Scientific reports*, 1--7.

Stein, G. H. (1979). T98G: An anchorage-independent human tumor cell line that exhibits stationary phase G1 arrest in vitro. *Journal of cellular physiology*, 43--54.

Stupp, R. a. (2005). Radiotherapy plus concomitant and adjuvant temozolomide for glioblastoma. *New England journal of medicine*, 987--996.

Sugiarto, S. a.-R. (2011). Asymmetry-defective oligodendrocyte progenitors are glioma precursors. *Cancer cell*, 328--340.

Szostecki, C. a. (1990). Isolation and characterization of cDNA encoding a human nuclear antigen predominantly recognized by autoantibodies from patients with primary biliary cirrhosis. *Journal of immunology (Baltimore, Md.: 1950)*, 4338--4347.

Terris, B. a.-F. (1995). PML nuclear bodies are general targets for inflammation and cell proliferation. *Cancer research*, 1590--1597.

Venkataramani, V. a. (2022). Glioblastoma hijacks neuronal mechanisms for brain invasion. *Cell, 185*, 2899--2917.

Verhaak, R. G. (2010). Integrated genomic analysis identifies clinically relevant subtypes of glioblastoma characterized by abnormalities in PDGFRA, IDH1, EGFR, and NF1. *Cancer cell*, 98--110.

Villagra, N. T.-B. (2006). The PML-nuclear inclusion of human supraoptic neurons: A new compartment with SUMO-1-and ubiquitin--proteasome-associated domains. *Neurobiology of disease*, 181--193.

Wirsching, H.-G. a. (2017). Glioblastoma. *Malignant Brain Tumors*, 265--288.

Zheng, H. a.-J. (2008). p53 and Pten control neural and glioma stem/progenitor cell renewal and differentiation. *Nature*, 1129--1133.

Zhong, S. a. (2000). The transcriptional role of PML and the nuclear body. *Nature cell biology*, E85--E90.

Zhu, Y. a. (2005). Early inactivation of p53 tumor suppressor gene cooperating with NF1 loss induces malignant astrocytoma. *Cancer cell*, 119--130.